The thermal excess in the X-ray spectra of accreting binary pulsars

Nicola La Palombara

Overview

- Summary on High Mass X-Ray Binaries
- HMXRBs in the Galaxy and in the Magellanic Clouds
- XMM observations of 4U 0352+309 and RX J0146.9+6121
- Thermal excess in X-ray Binary Pulsars
- Origin of the thermal component
- Future work

High Mass X-Ray Binaries

Components:

- a compact accreting stellar object (NS or BH)
- a high mass donor star (OB supergiant or Be)

X-ray variability:

- persistent bright sources ($L_X > 10^{36}$ erg s^{-1})
- transient sources: quiescent phases ($L_X < 10^{35}$ erg s^{-1}) interrupted by intense ($L_X > 10^{36}$ erg s^{-1}) outbursts
- persistent low-luminosity sources ($L_X \sim 10^{34-35}$ erg s^{-1})

Several HMXRBs show pulsed emission, with P = 0.03-10000 s

Be X-Ray Binaries

Dominant population of HMXRBs in the Milky Way and in the Magellanic Clouds

Elliptical orbits with eccentricities e = 0.1-0.9 and P_{orb} = 17-263 d

Optical component not evolved (luminosity class III-V) => smaller than its Roche lobe

Be star surrounded by an extended circumstellar envelope of ionized gas (*decretion disc*), which disperses and refills on time scales ~ years and is truncated by the orbiting NS (relation H_{α} - P_{orb})

- emission lines and IR excess compared to normal B stars
- rotationally dominated disc; fast radiative wind in the polar regions and slow high density outflow in the equatorial regions

Typical Be X-Ray Binaries....

Transient nature of the X-ray emission controlled by the *centrifugal gate* mechanism (operated both by the periastron passages and by the dynamical evolution of the decretion disc)

Two types of outbursting activity:

- Type I: periodic outbursts due to periastron transit of the NS; short duration (0.2-0.3 P_{orb}); peak luminosities $L_X \sim 10^{37}$ erg s^{-1}
- Type II: aperiodic outburst due to decretion disc instability; long duration (up to several P_{orb}); peak luminosities $L_X \sim 10^{38}$ erg s^{-1} ($\sim L_{EDD}$); possible formation of an accretion disc (pulsar spin-up)

Hard spectrum (kT>15 keV, E_{cut}=10-20 keV) => hard X-ray transients

...and persistent Be X-Ray Binaries

Classification by Reig & Roche (1999):

- persistent low luminosity ($L_X \sim 10^{34-35}$ erg s^{-1}) with small fluctuations
- no outbursts
- long pulse periods ($P_{spin} > 200$ s)
- low cut-off energy (~4 keV instead of 10-20 keV)
- absence or very weak Iron line at 6.4 keV

- $P_{spin} \sim P_{orb}^2$ (Corbet 1986) => large orbits ($P_{orb} > 100$ d)
  => accretion from low density regions
- no outbursts => low eccentricity

no tidal circularisation => primordial low eccentricity

↓

<u>low kick velocity at birth for the NS</u>

An increasing family...

Several HMXRBs discovered in the latest years in the Magellanic Clouds: 92 in the SMC and 36 in the LMC (Liu et al., 2005)

- small angular size
- close and known distance
- low absorption due to high Galactic latitude

Galaxy	HMXBs	
	Total	Pulsar
SMC	92	47
SMC∗100	9200	4700
LMC	36	7
LMC∗10	360	70
Galaxy	108	57

Overabundant population of HMXRBs in the SMC relative to the MW

Unusually high concentration of BeXRB systems in the SMC (> 90 % of all the HMXRBs, compared to 60-70 % in MW and LMC), in a region of recent (< 30 My) star formation

An increasing family...

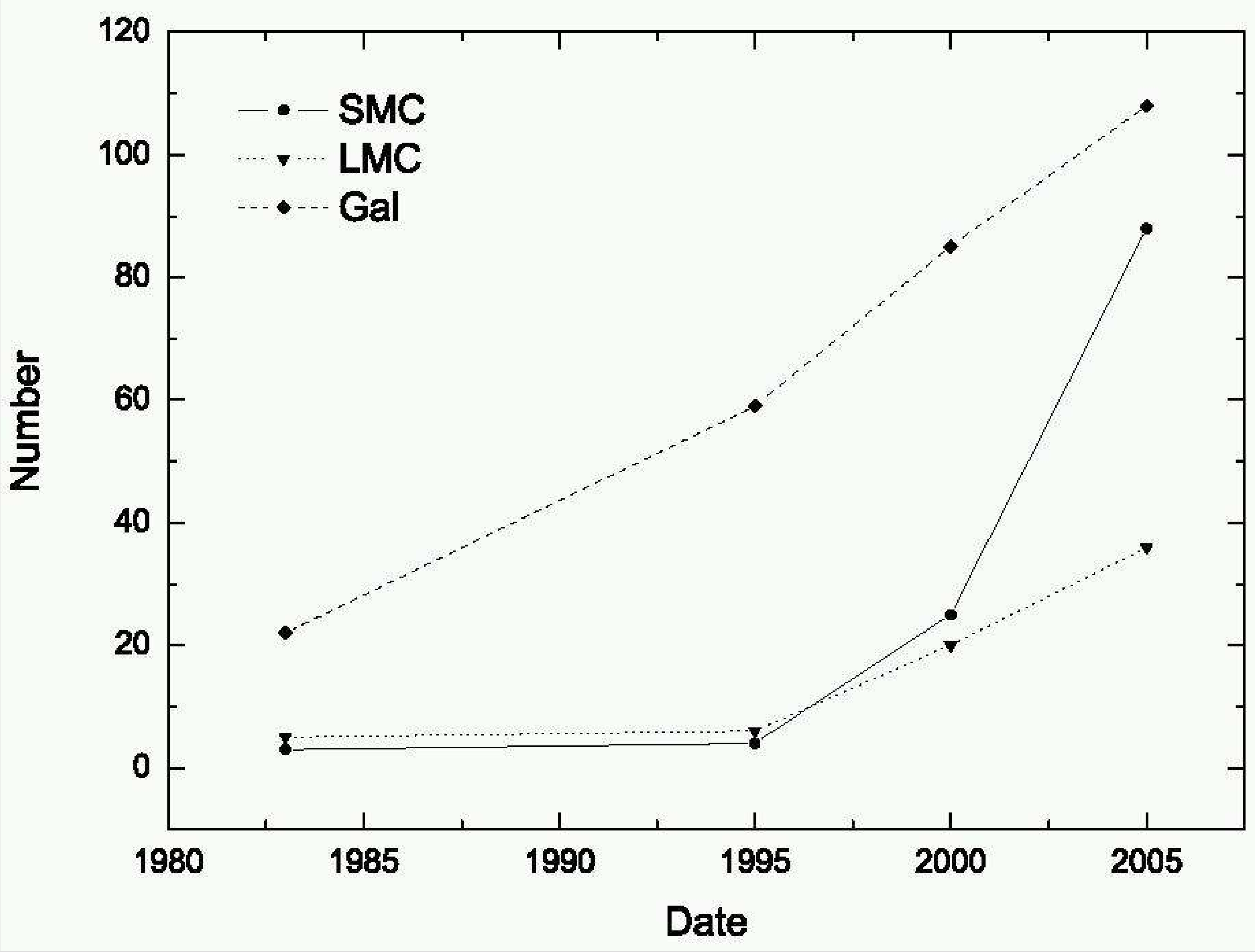

Liu et al., 2005

An increasing family...

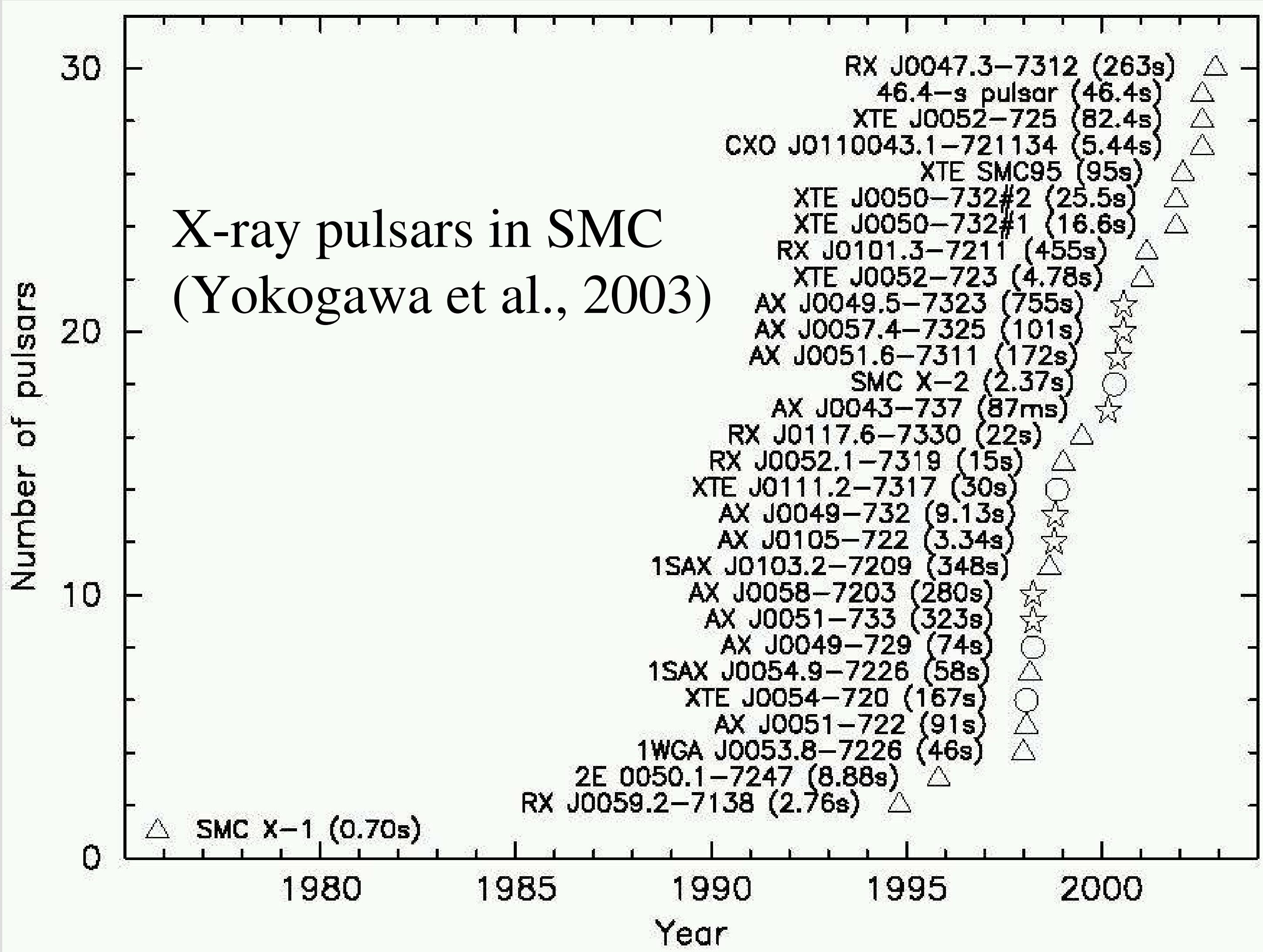

An increasing family...

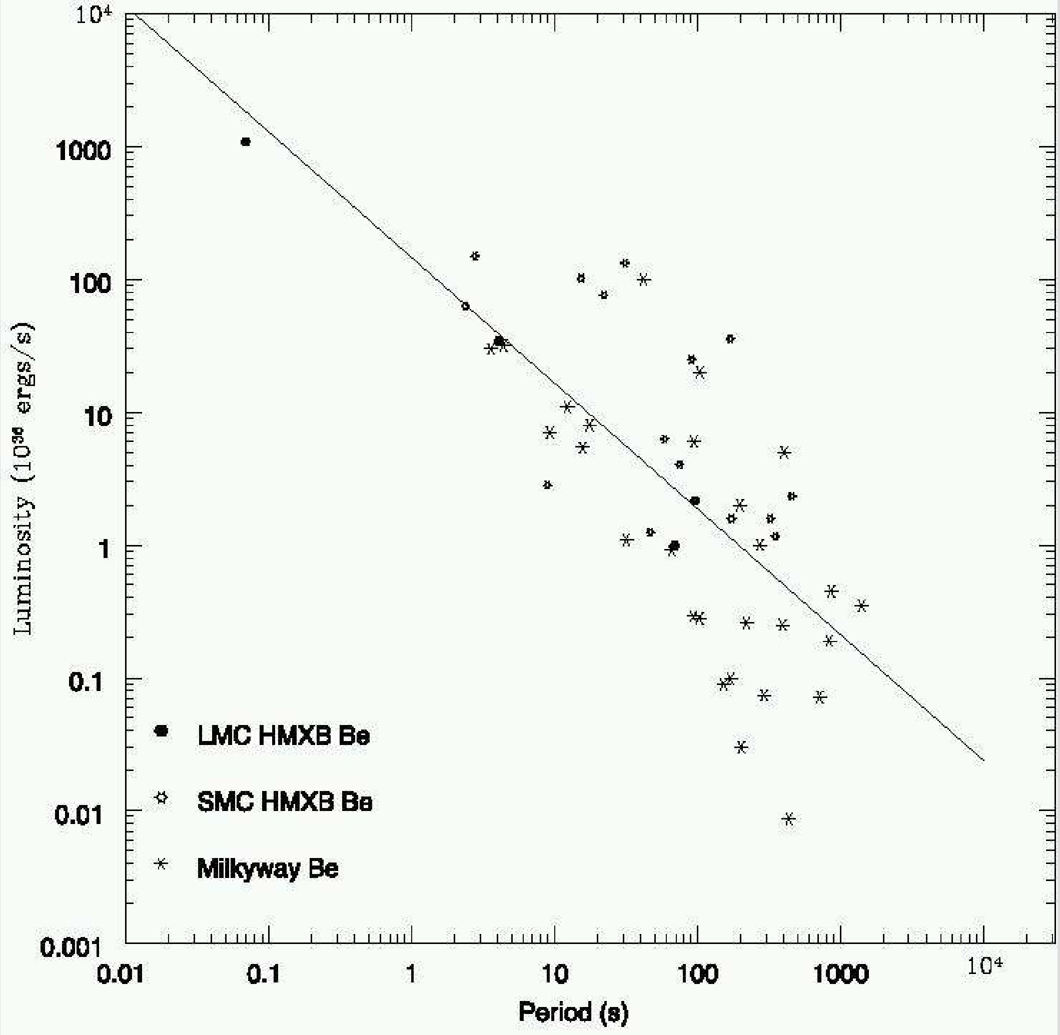

Inverse correlation between maximum X-ray flux density and spin period, due to accretion physics:

- accretion rate ~ $1/r^n$, n ~ 3
- r ~ $P_{orb}^{2/3}$
- P_{spin} ~ P_{orb}^2

=> L ~ P_{spin}^{-1}

Majid et al., 2004

XMM observation of two persistent BeXBRs

X-ray source	4U 0352+309	RX J0146.9+6121
Luminosity (2-10 keV)	~10^{35} erg s^{-1}	~10^{34} erg s^{-1}
Pulse period	839.3 ± 0.3 s	1396.1 ± 0.2 s
Orbital period	250.3 d	?
Orbital eccentricity	0.11	?
Optical counterpart	X Persei	LS I +61^{o} 235
Spectral type	O9.5 IIIe	B0 IIIe
Source distance	0.95 kpc	~ 2.5 kpc

Folded light curves

4U 0352+309

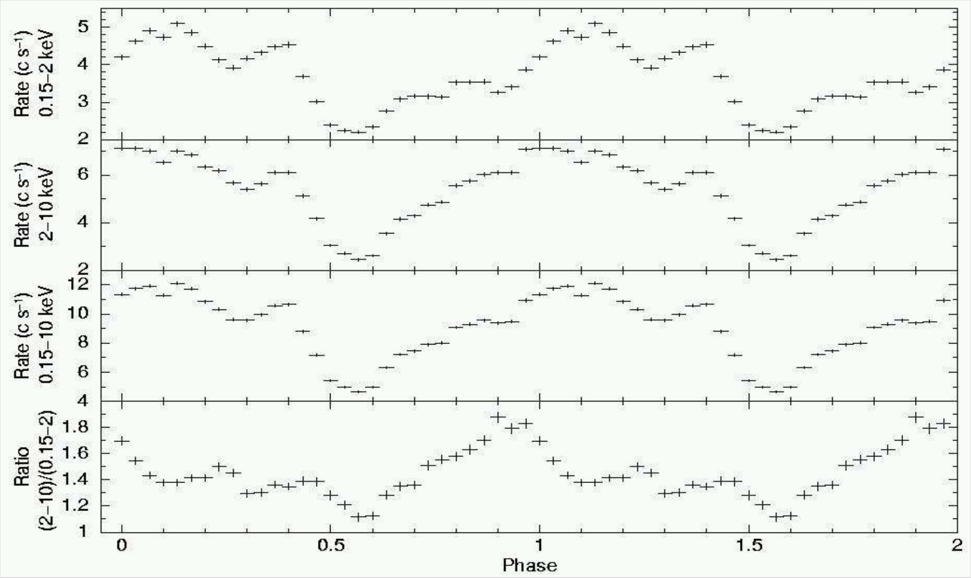

RX J0146.9+6121

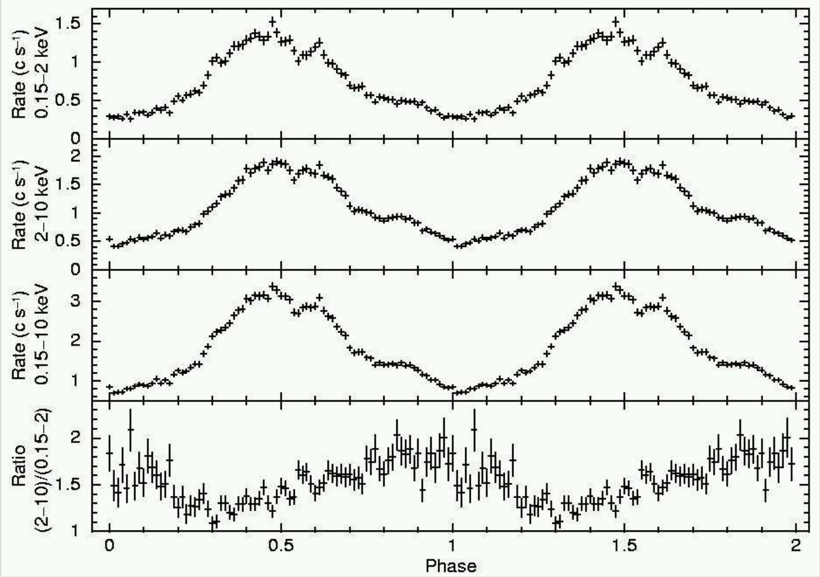

=> the pulse profile is energy dependent

=> the pulse shape is not simply sinusoidal

Timing analysis - 4U 0352+309

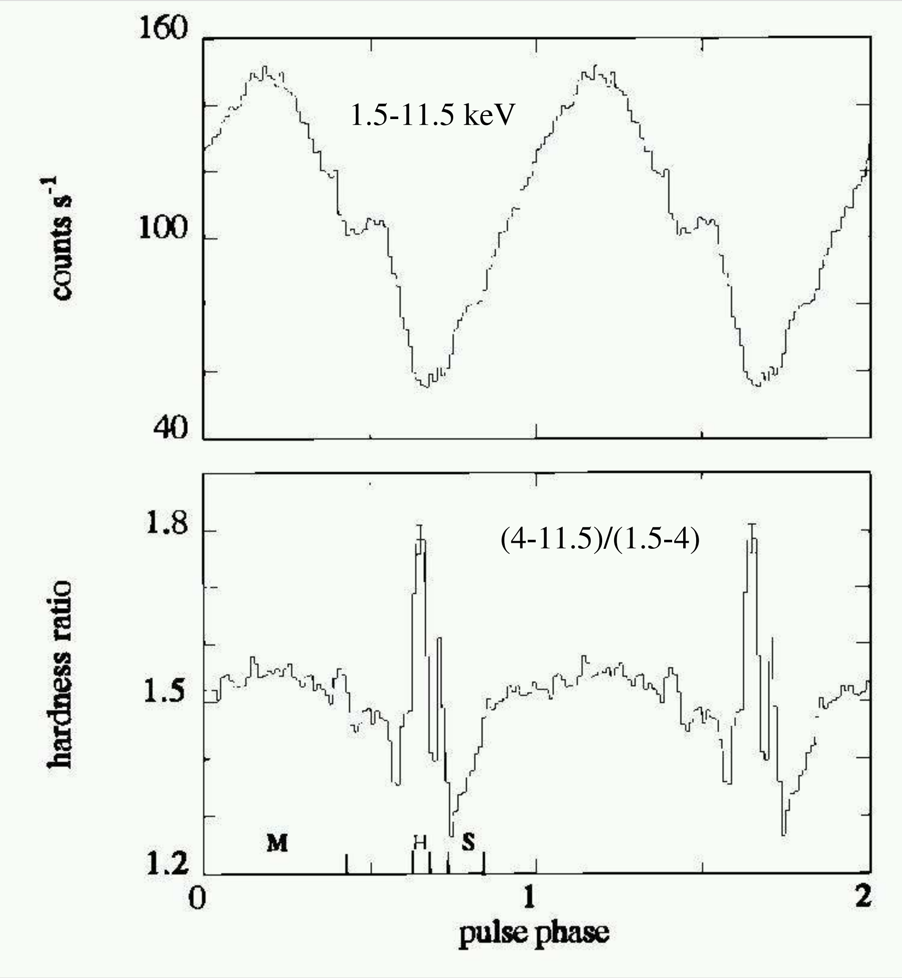

GINGA (Robba et al., 1996)

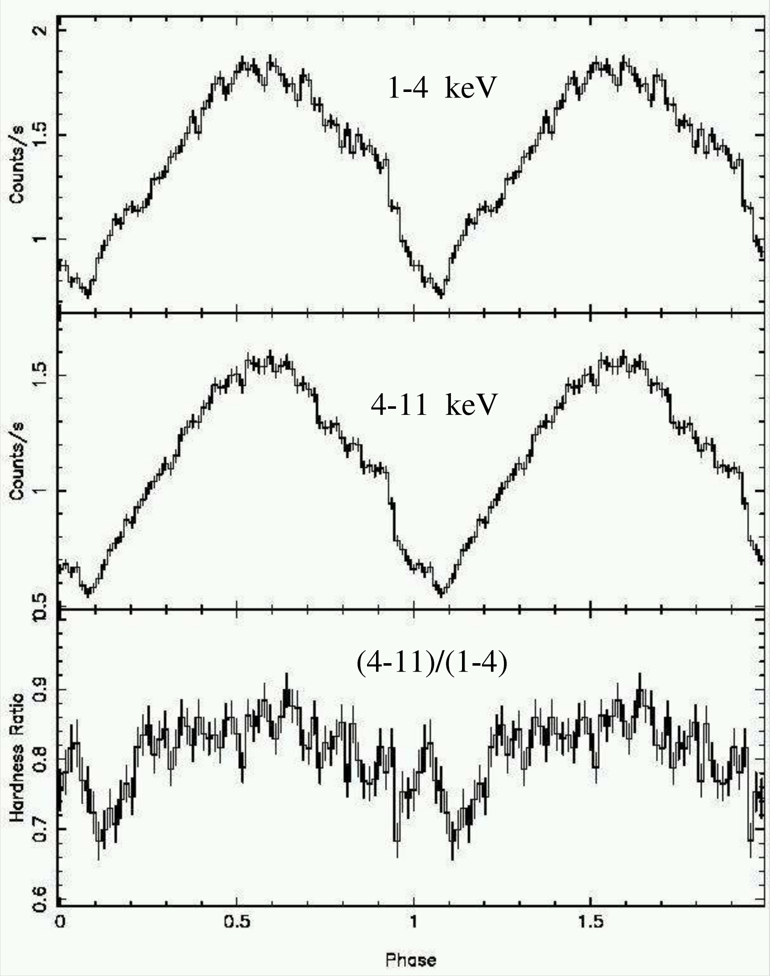

SAX (Di Salvo et al., 1998)

Timing analysis - 4U 0352+309

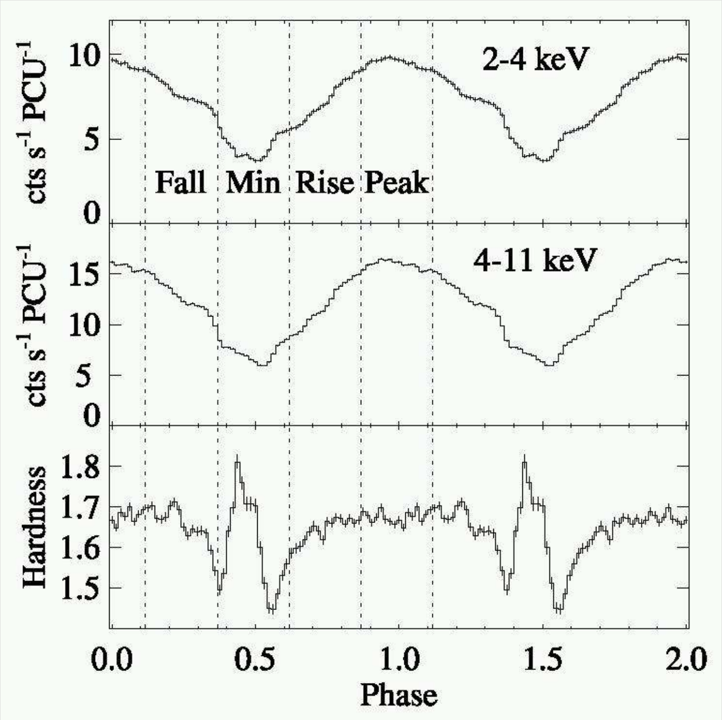

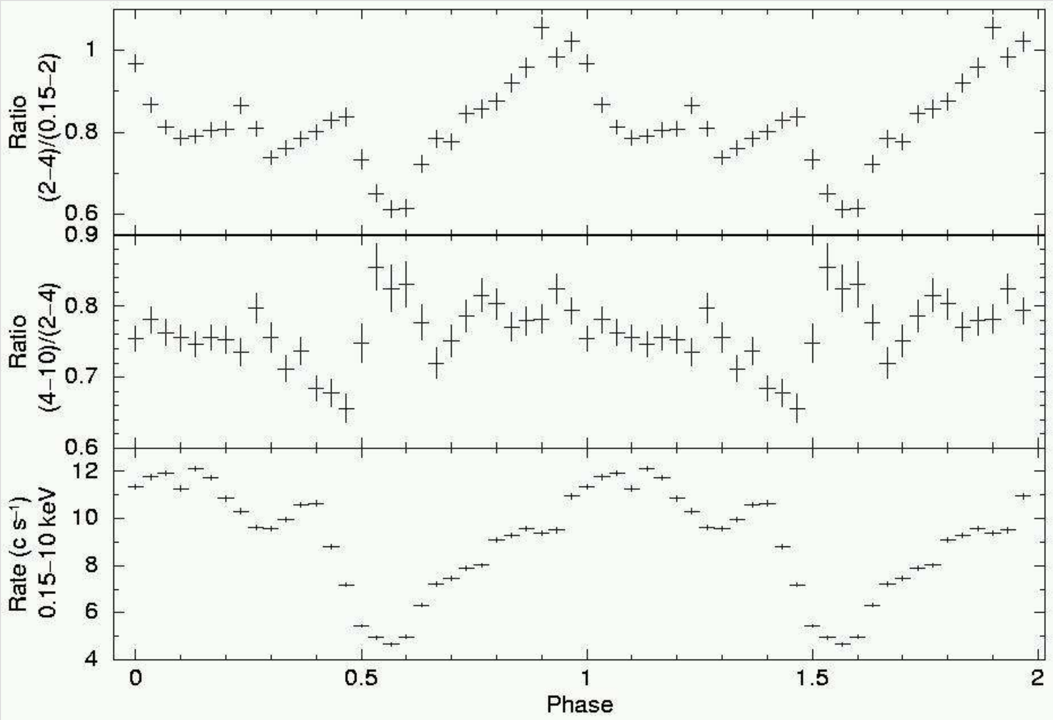

RXTE (Coburn et al., 1998) XMM (La Palombara & Mereghetti, 2007)

↓

The opposite behaviour of the two HRs reveals a complex spectral evolution

Timing analysis - RX J0146.9+6121

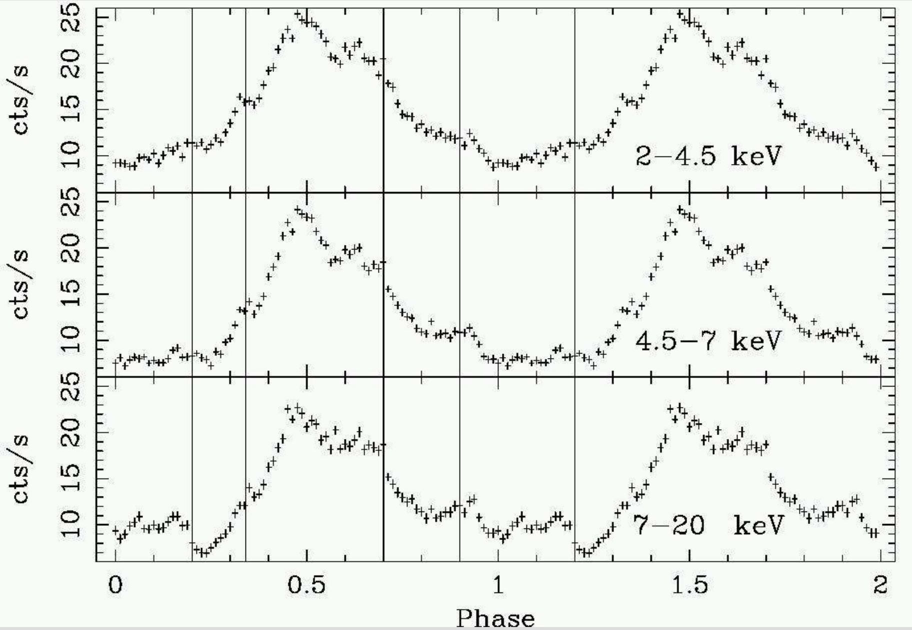

RXTE (Mereghetti et al., 2000)

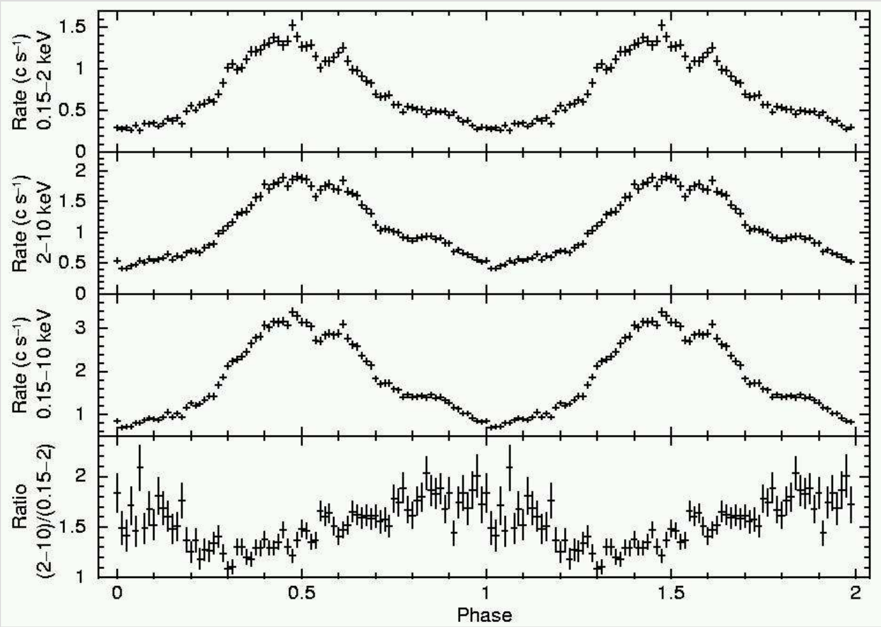

XMM (La Palombara & Mereghetti, 2006)

↓

detection of pulsed emission also below 2 keV

Phase-averaged spectra - I

4U 0352+309 | RX J0146.9+6121

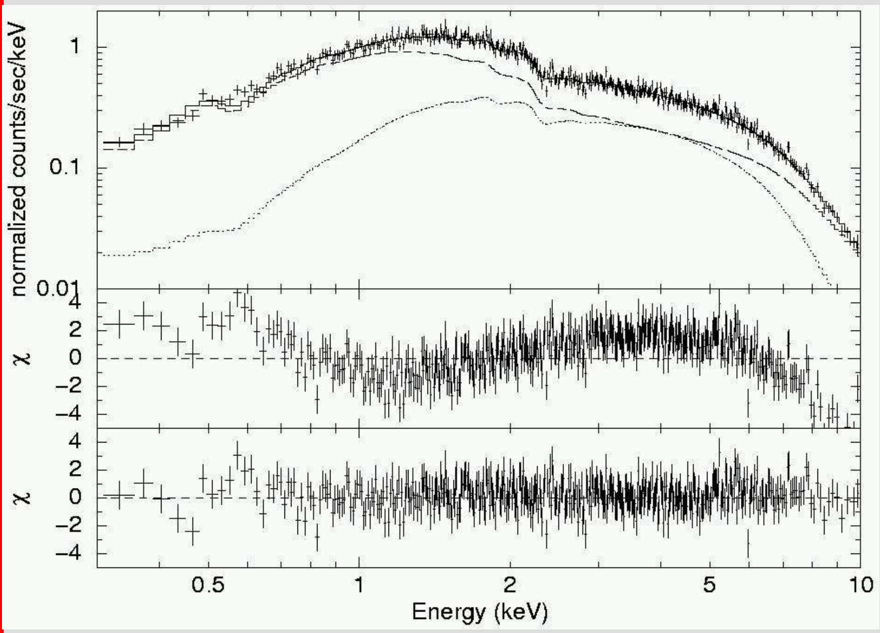

PL

PL+BB

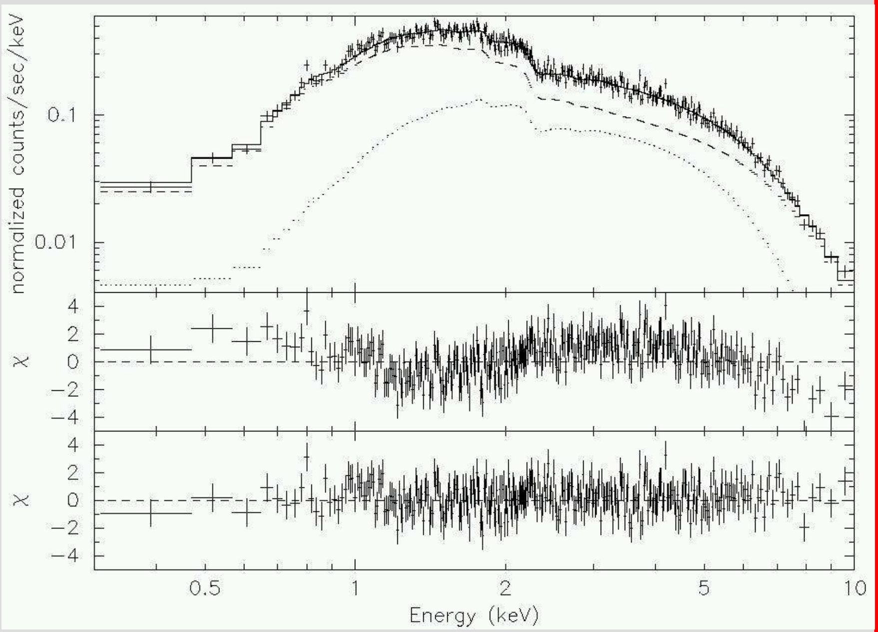

=> a single power-law component does not describe the observed spectra

=> the addition of a black-body component improves the fit quality

=> no evidence of an Iron line between 6 and 7 keV

Phase-averaged spectra - II

X-ray source	4U 0352+309	RX J0146.9+6121
Photon index	1.48 ± 0.02	1.34 ± 0.05
Black-body temperature (keV)	1.42 ± 0.03	1.11 ± 0.06
Black-body radius (m)	361 ± 3	140 ± 15
Luminosity (0.3-10 keV, erg s^{-1})	$\sim 1.4 \times 10^{35}$	$\sim 1.5 \times 10^{34}$
Flux PL (%)	~ 61	~ 76
Flux BB (%)	~ 39	~ 24
Upper Limit EQW Fe (keV)	~ 0.1	~ 0.15

Phase-averaged spectra - 4U 0352+309

Observation	XMM (2003)	RXTE (1998)
Photon index	1.48 ± 0.02	1.83 ± 0.03
Black-body temperature (keV)	1.42 ± 0.03	1.48 ± 0.02
Black-body radius (m)	361 ± 3	130 ± 30
Luminosity (2-10 keV, erg s^{-1})	$\sim 1 \times 10^{35}$	$\sim 2 \times 10^{34}$
Flux PL (%)	~ 56	~ 65
Flux BB (%)	~ 44	~ 35

↓

BB temperature and contribution to the total flux independent of the source luminosity

Phase-resolved spectroscopy - I

4U 0352+309

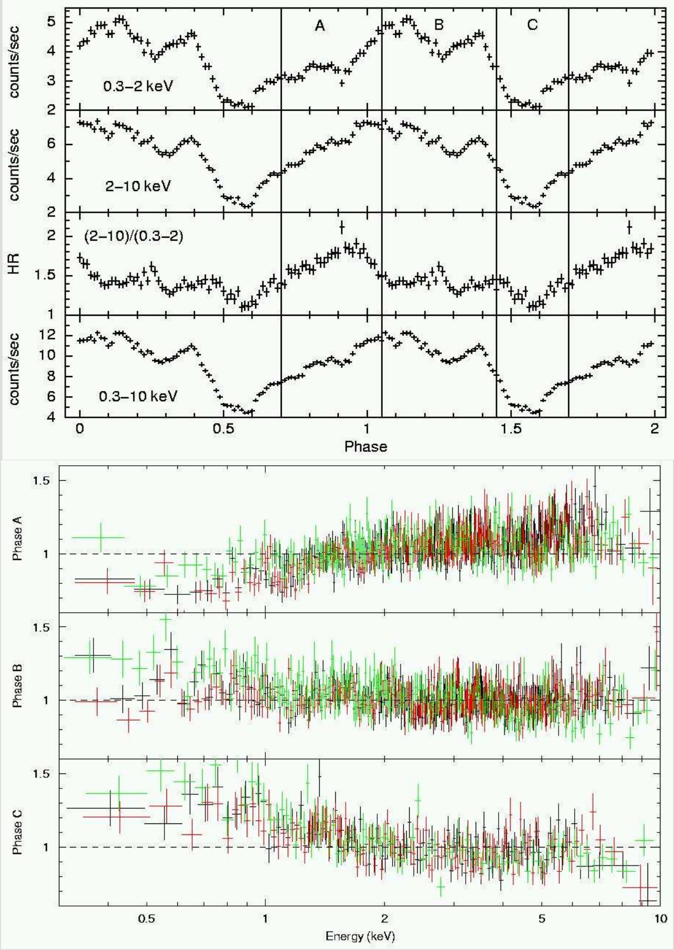

RX J0146.9+6121

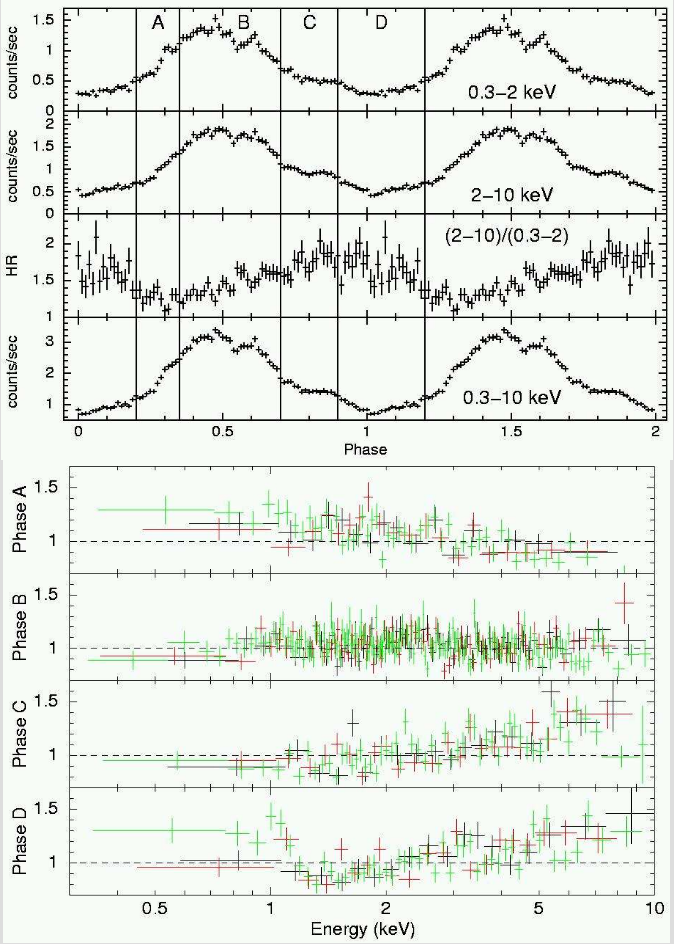

spectral variability with the pulse phase

Phase-resolved spectroscopy - II

4U 0352+309

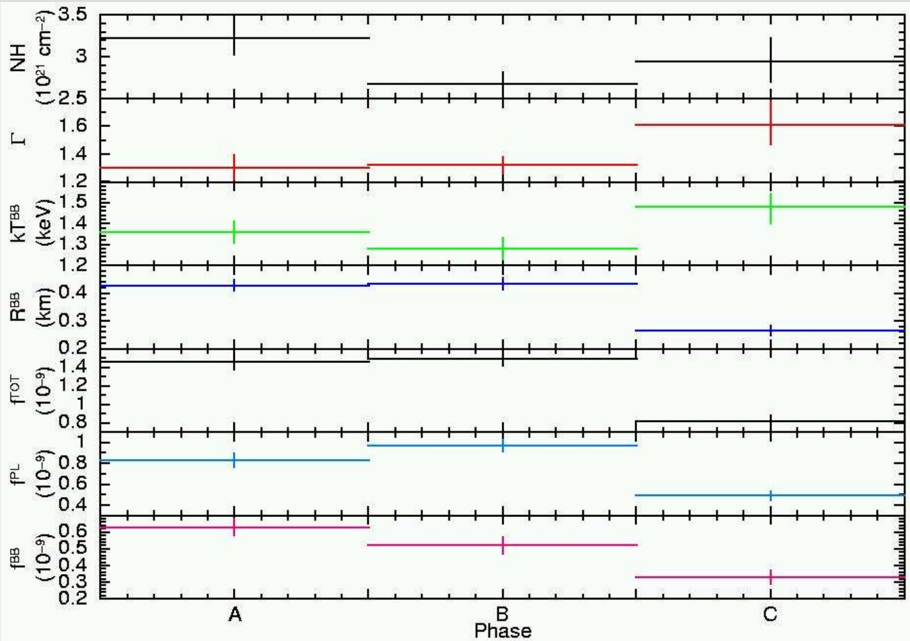

RX J0146.9+6121

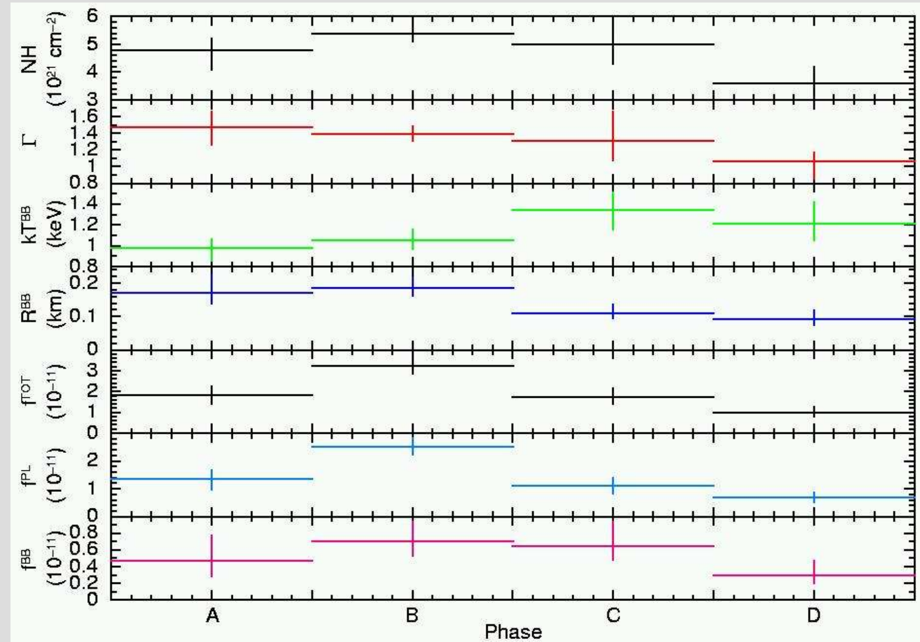

- N_H nearly constant along the pulse phase => interstellar extinction
- Γ variations only at the pulse minimum
- Significant variations of the BB Temperature and Radius
- Variations of the total flux, but ~ constant BB fraction along the pulse phase

Phase-resolved spectroscopy - III

4U 0352+309

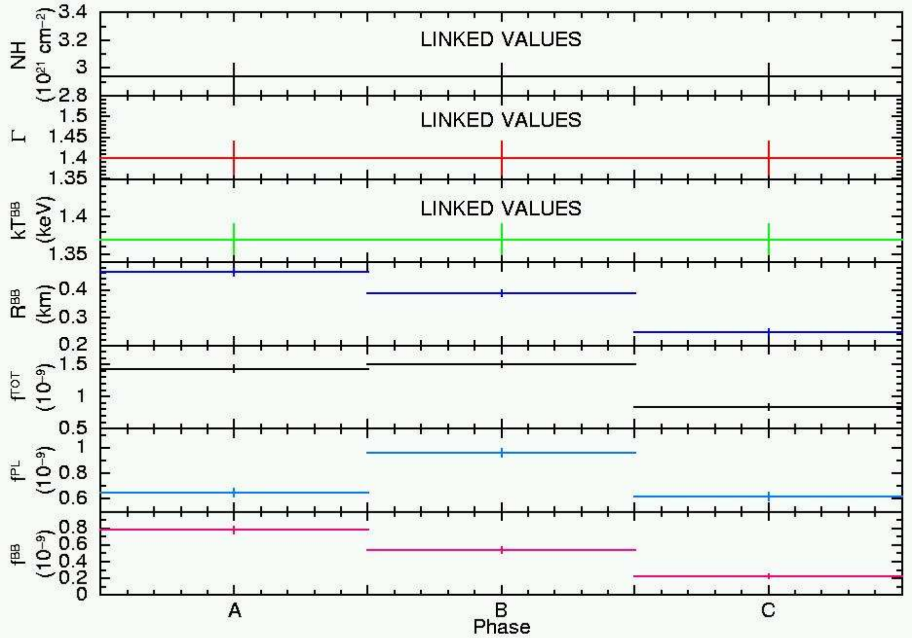

RX J0146.9+6121

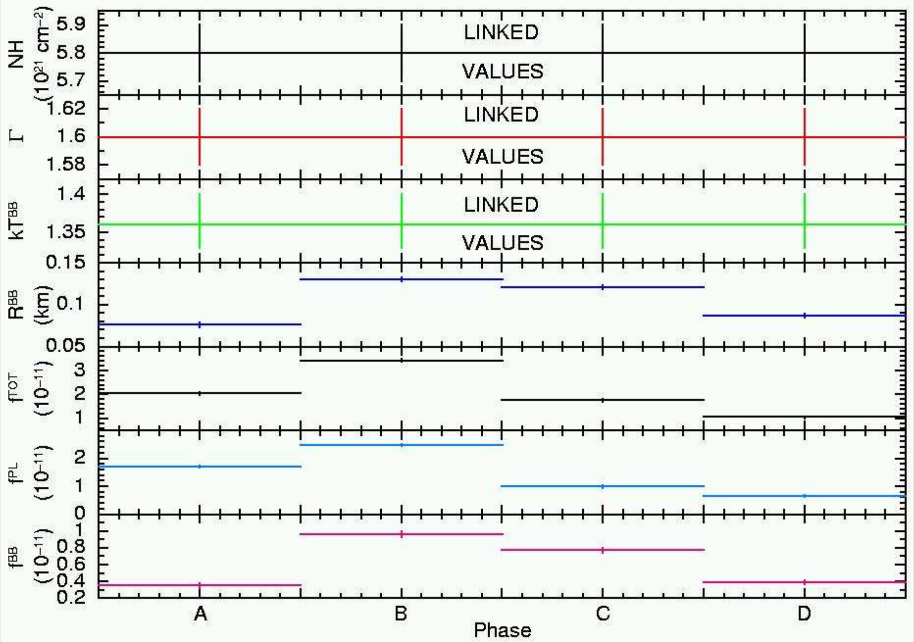

forced common values for N_H, Γ and kT_{BB}

↓

variations in the relative contribution of the PL and BB components

↓

evidence that the BB component is really variable?

Phase-resolved spectroscopy - IV

4U 0352+309

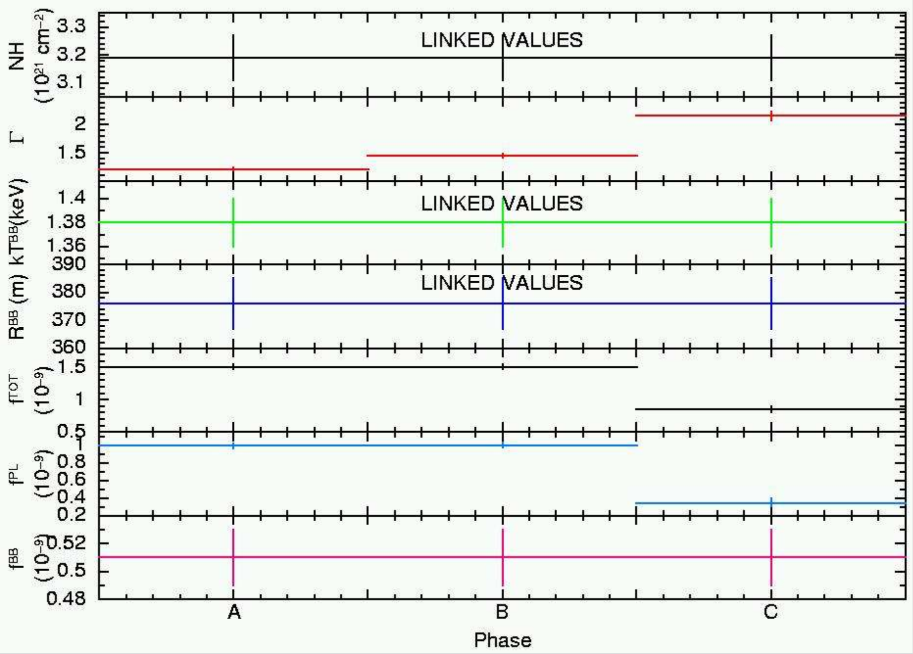

RX J0146.9+6121

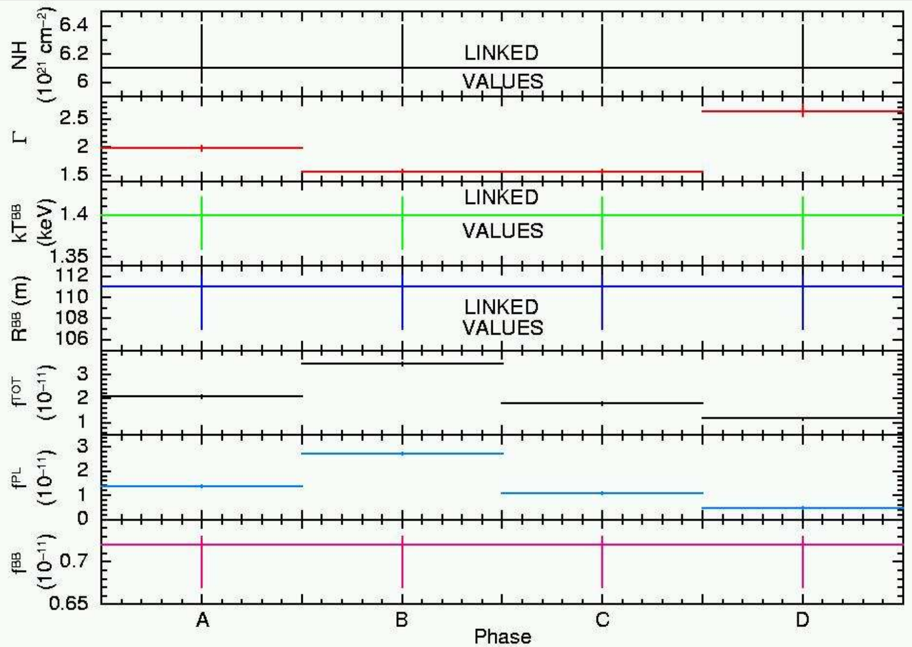

a constant BB component is not rejected by the data

↓

<u>the spectral variability can be attributed to the PL component</u>

Luminosity and pulse period history

4U 0352+309

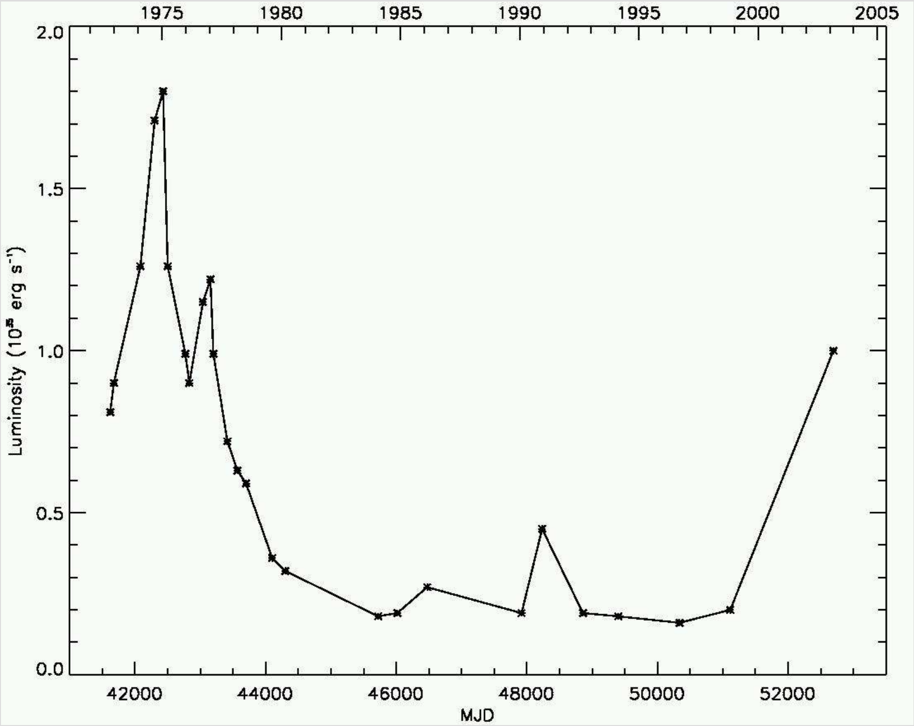

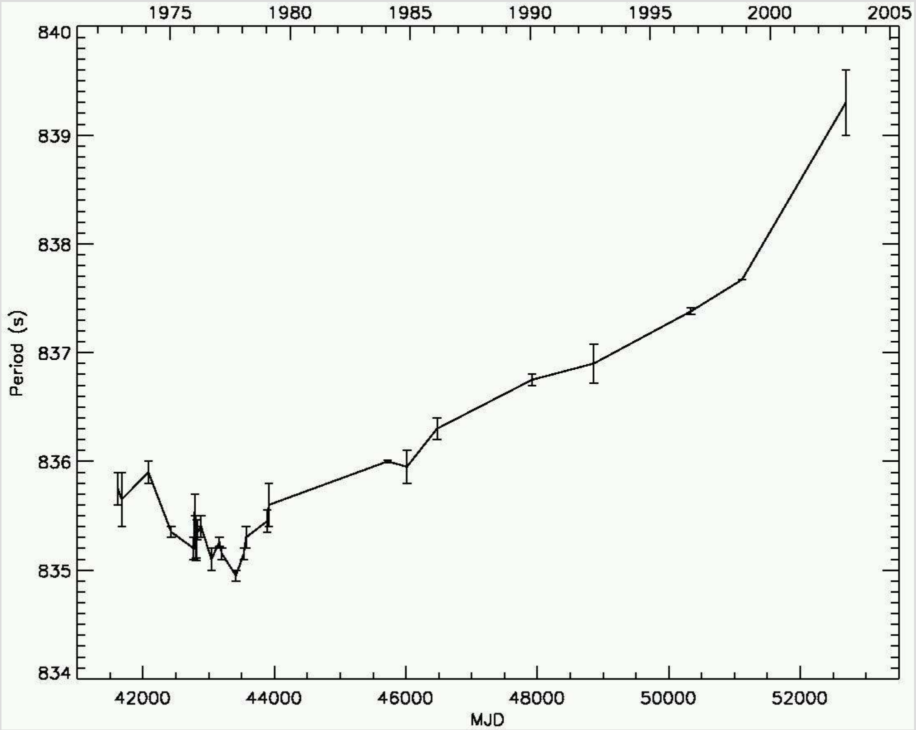

the pulsar spin-down has proceeded also during the luminosity increase

↓

<u>no evidence of accretion disc</u>

Luminosity and pulse period history

RX J0146.9+6121

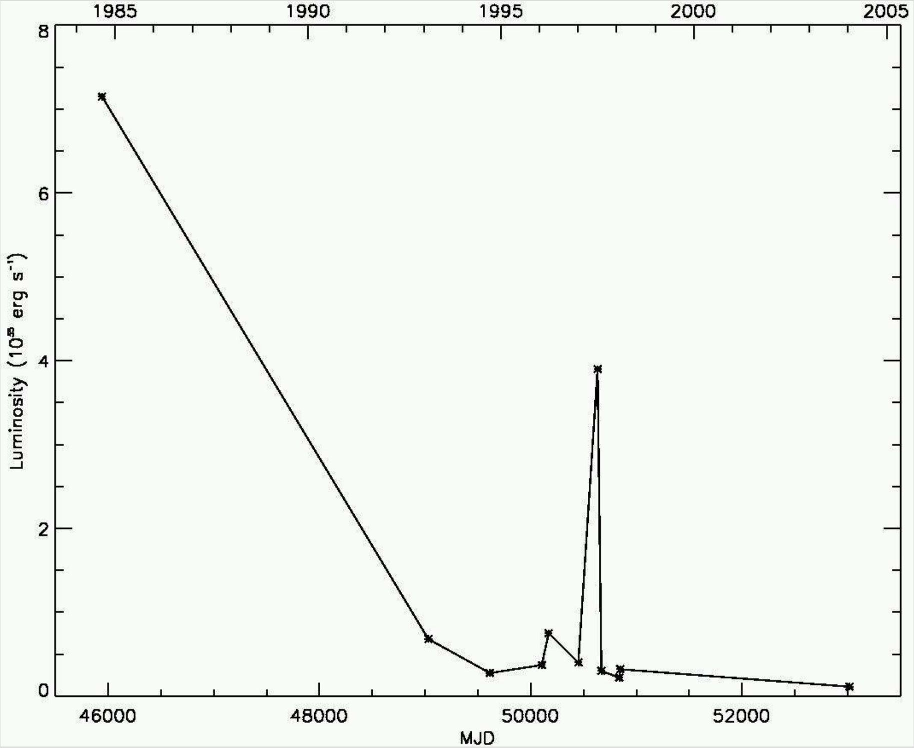

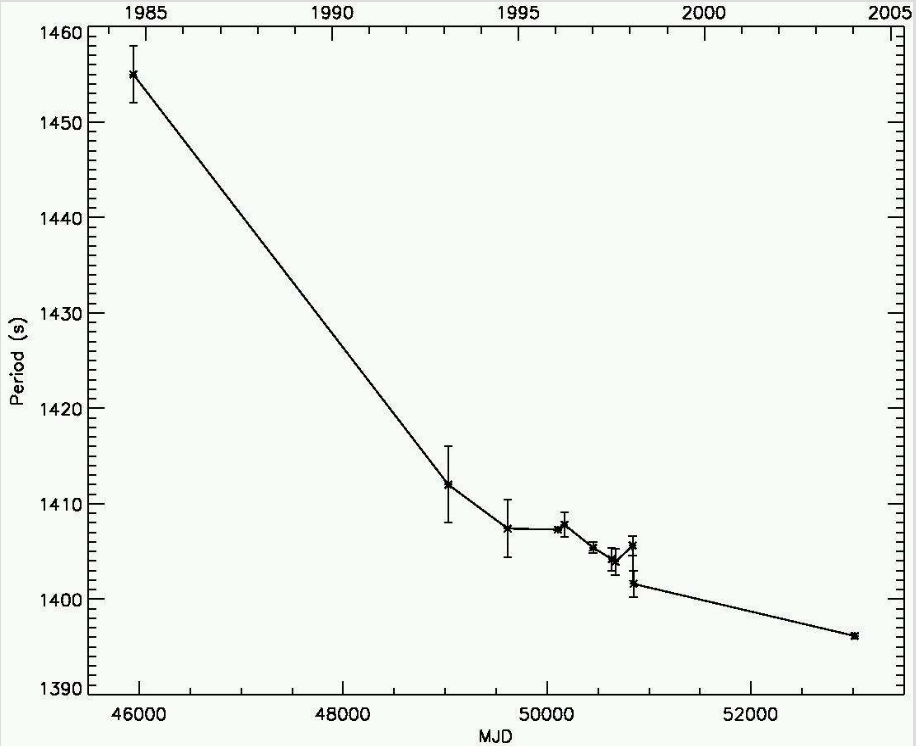

in spite of the source decreasing luminosity, the pulsar is still in a spin-up phase

↓

momentum transfer to the NS even with low accretion rates

Common properties of 4U 0352+309 and RX J0146.9+6121

Persistent sources

Low luminosity ($L_X < 10^{36}$ erg s^{-1})

Long pulse period (P > 100 s)

Data excess over the main PL component of BB type

High BB temperature (kT > 1 keV)

Small emission area (R < 0.5 km)

~ 30 % of the total flux due to the thermal component

X-ray Binary Pulsars with an observed data excess

La Palombara & Mereghetti, 2006

Source[a]	Location	Distance (kpc)	Companion Star	P_{pulse} (s)	L_X^b (ergs s^{-1}, keV)	Flux (ergs cm^{-2} s^{-1})	N_H^c (10^{21} cm^{-2})	L_{SE}/L_X	SE model[d]	kT_{BB} (keV)	SE Pulses[e]
Her X–1[1]	Galaxy	$\sim$5	A7 V	1.24	1.0×10^{37} (0.3-10)	3.3×10^{-9}	0.05	0.04–0.10	BB, BB+LE	0.09–0.12	Yes
SMC X–1[2]	SMC	65	B0 Ib	0.7	2.4×10^{38} (0.7–10)	4.7×10^{-10}	2–5	0.036	BB, TB, SPL	0.15–0.18	Yes
LMC X–4[3]	LMC	50	O7 III–O IV	13.5	1.2×10^{38} (0.7–10)	4.0×10^{-10}	$\sim$0.5	0.064	BB, BB+TB, COM, SPL	0.15	Yes
XTE J0111.2–7317[4]	SMC	65	B1 IVe	30.95	1.8×10^{38} (0.7–10)	3.6×10^{-10}	1.8	$\sim$0.10	SPL	...	Yes
RX J0059.2–7138[5]	SMC	65	B1 IIIe	2.76	2.6×10^{38} (0.1–10)	5.1×10^{-10}	0.42–0.50	0.31	MEK, SPL	...	No
4U 1626–67[6]	Galaxy	?	Low–mass	7.7	$2.6 \times 10^{34} D^2_{kpc}$ (0.5-10)	2.2×10^{-10}	0.6	0.10	BB	0.34	No
Cen X–3[7]	Galaxy	$\sim$8	O6–O8 II	4.8	2.4×10^{38} (0.1–10)	3.2×10^{-8}	19.5	$\sim$0.7	BB	0.11	Yes
Vela X–1[8]	Galaxy	1.9	B0.5 Ib	283	2.2×10^{36} (2–10)	5.1×10^{-9}	4.2	$\sim$0.01	TB	...	No
X Per[9]	Galaxy	0.95	O9.5pe	837	1.8×10^{34} (0.3–10)	1.7×10^{-10}	1.5	0.24	BB	1.45	?
EXO 053109–6609.2[10]	LMC	50	B0.7 Ve	13.7	4.6×10^{37} (0.2–10)	1.5×10^{-10}	6.9	?	MEK+PL	...	Yes
A 0538–66[11]	LMC	50	B2 IIIe	0.069	4.0×10^{37} (0.1–2.4)	1.3×10^{-10}	0.8	?	BB, TB	$\sim$0.2	?
RX J0047.3-7312[12]	SMC	65	B2e	263	$1.5, 2 \times 10^{36}$ (0.7–10)	$3.0, 4.0 \times 10^{-12}$	0.96,3.4	0.03–0.09,0.68	BB	0.6, 2.2	Yes
RX J0101.3-7211[13]	SMC	65	Be	452	1.6×10^{35} (0.3–10)	3.2×10^{-13}	0.6	?	MEK	...	?
RX J0103.6-7201[14]	SMC	65	O5 Ve	1323	$0.8 - 7.5 \times 10^{36}$ (0.2–10)	$1.6 - 14.8 \times 10^{-12}$	1.9	?	MEK	...	No
AX J0049.5-7323[15]	SMC	65	B2 Ve	751	$7 - 9 \times 10^{35}$ (0.2–10)	$1.4 - 1.8 \times 10^{-12}$	3.6	?	?	...	Yes
AX J0058-720[13]	SMC	65	Be	281	1.2×10^{35} (0.3–10)	2.4×10^{-13}	0.6	?	?	...	Yes
AX J0103-722[13]	SMC	65	B0 IV	342	1.8×10^{35} (0.3–10)	3.6×10^{-13}	0.6	?	MEK	...	?
3A 0535+262[16]	Galaxy	2.0	O9.7 IIIe	103.4	3.9×10^{33} (2–10)	8.2×10^{-12}	6.0	0.35	BB	1.33	?
RX J0146.9+6121	Galaxy	2.5	B0 IIIe	1395	1.5×10^{34} (0.3–10)	2.0×10^{-11}	5.1	0.25	BB	1.11	?

[a] References: (1) dal Fiume et al. (1998), Endo et al. (2000), Ramsay et al. (2002); (2) Woo et al. (1995), Paul et al. (2002); (3) Woo et al. (1996), La Barbera et al. (2001), Naik & Paul (2004); (4) Yokogawa et al. (2000b); (5) Kohno et al. (2000); (6) Schulz et al. (2001); (7) Burderi et al. (2000); (8) Haberl (1994), Orlandini et al. (1998), Kreykenbohm et al. (2002); (9) di Salvo et al. (1998), Coburn et al. (2001); (10) Haberl et al. (2003); (11) Mavromatakis & Haberl (1993); (12) The two set of values are base on Ueno et al. (2004) and Majid et al. (2004), respectively; (13) Sasaki et al. (2003); (14)Sasaki et al. (2003), Haberl & Pietsch (2005); (15) Yokogawa et al. (2000a), Haberl & Pietsch (2004); (16) Mukherjee & Paul (2005).

[b] For each source the reference energy range is also reported.

[c] The reported values refer only to the interstellar absorption, not to the source intrinsic absorption.

[d] Spectral models used for the soft excess are: BB = blackbody; TB = thermal bremsstrahlung; SPL = soft power–law or broken power–law; MEK = MEKAL thin thermal model; COM = Comptonization model; LE = broad low–energy line emission. Commas indicate separate fits, plus signs indicate fits with two components.

[e] Pulsation of the emission component that traces the soft excess.

the soft/thermal component can be a common feature intrinsic to accreting X-ray pulsars

Her X-1

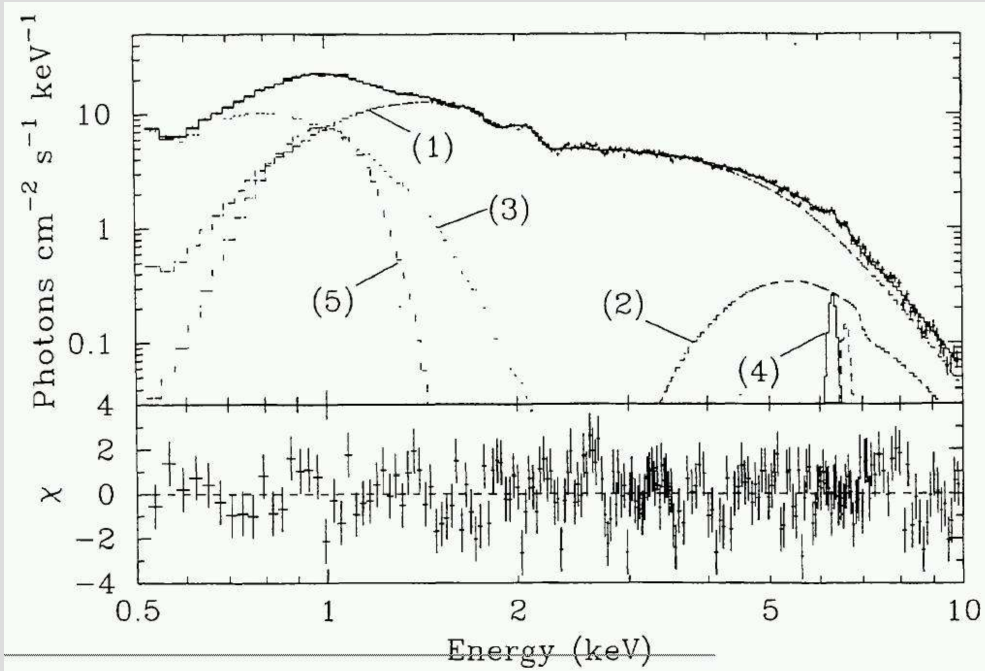

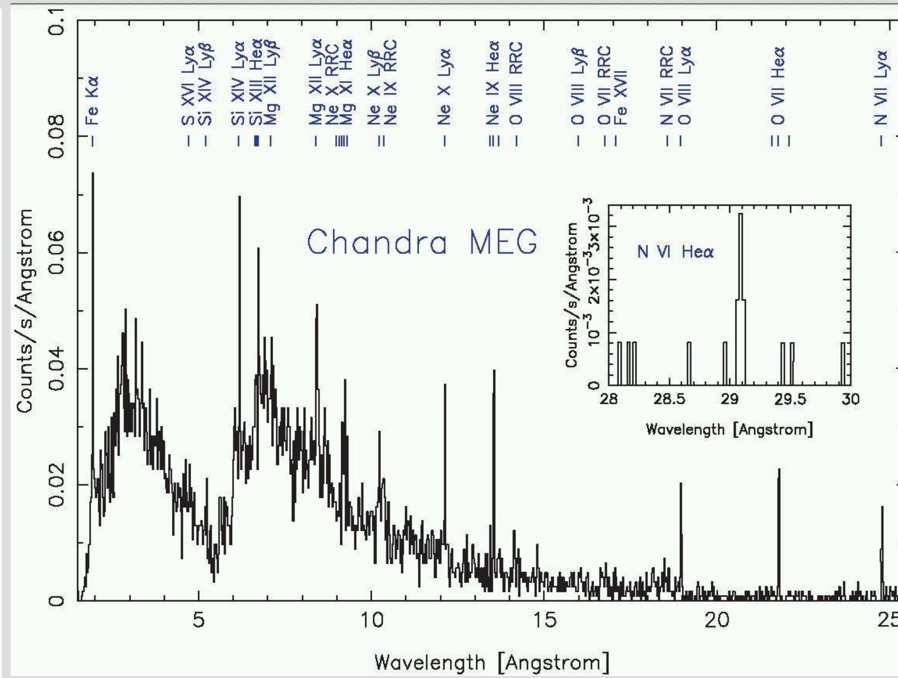

ASCA - Endo et al., 2000
kT_{BB} = 0.16 keV
L_X(0.1-10) = 1.8 x 10^{37} erg s^{-1}

Chandra - Jimenez-Garate et al., 2005
PL+BB, kT_{BB} = 0.18 keV
L_X(0.1-10) = 2.5 x 10^{35} erg s^{-1}

4U 1626-67

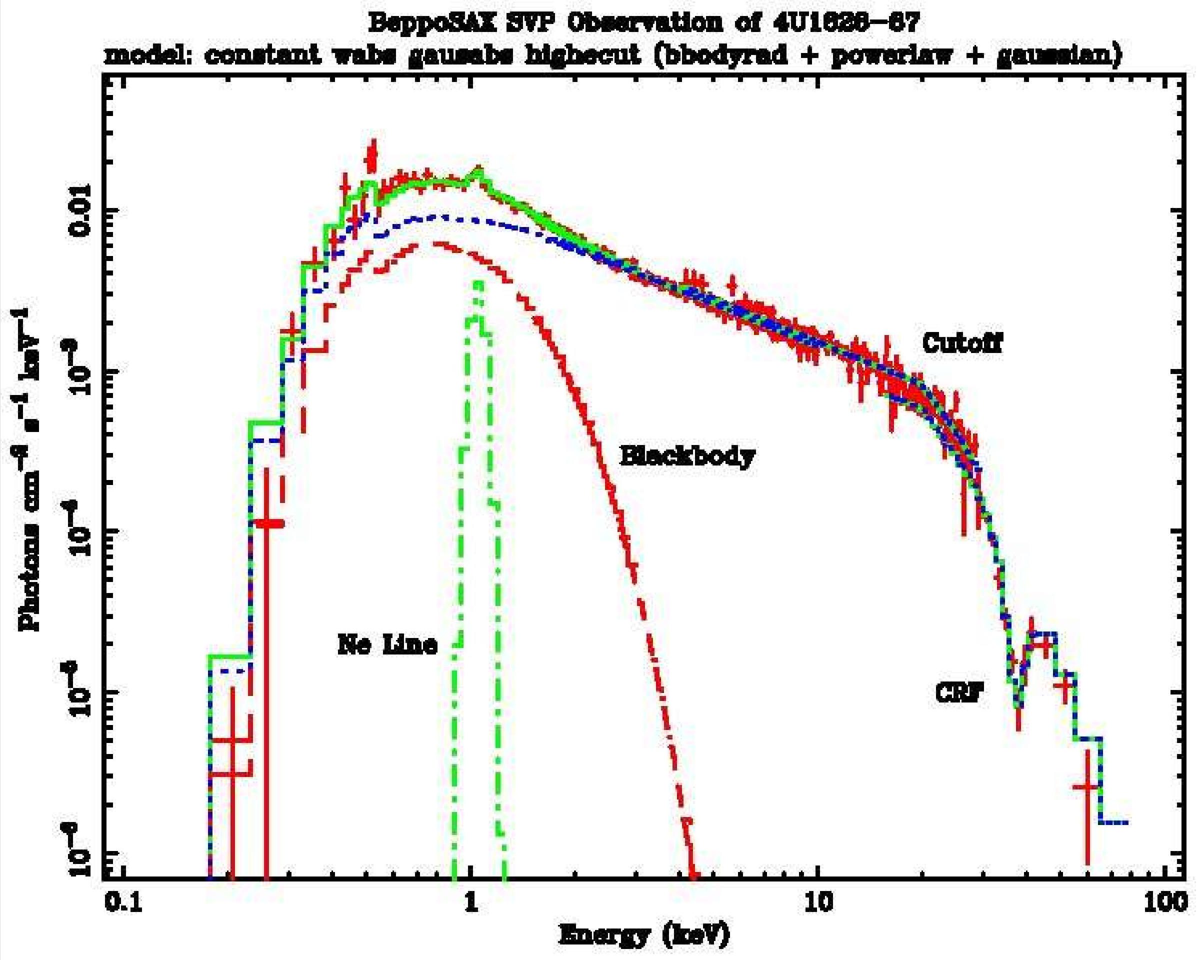

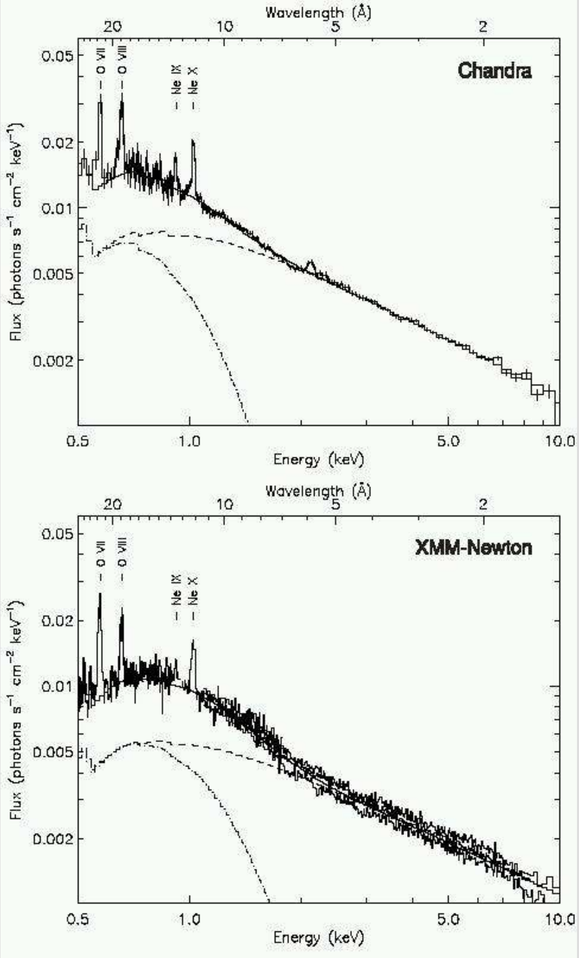

Orlandini et al., 1998:
$kT_{BB} = 0.29$ keV, $L_X(0.1\text{-}200) = 7.7 \times 10^{34}\, d_{kpc}^2$ erg s^{-1}

Krauss et al., 2007:
PL+BB, $kT_{BB} = 0.25$ keV

LMC X-4

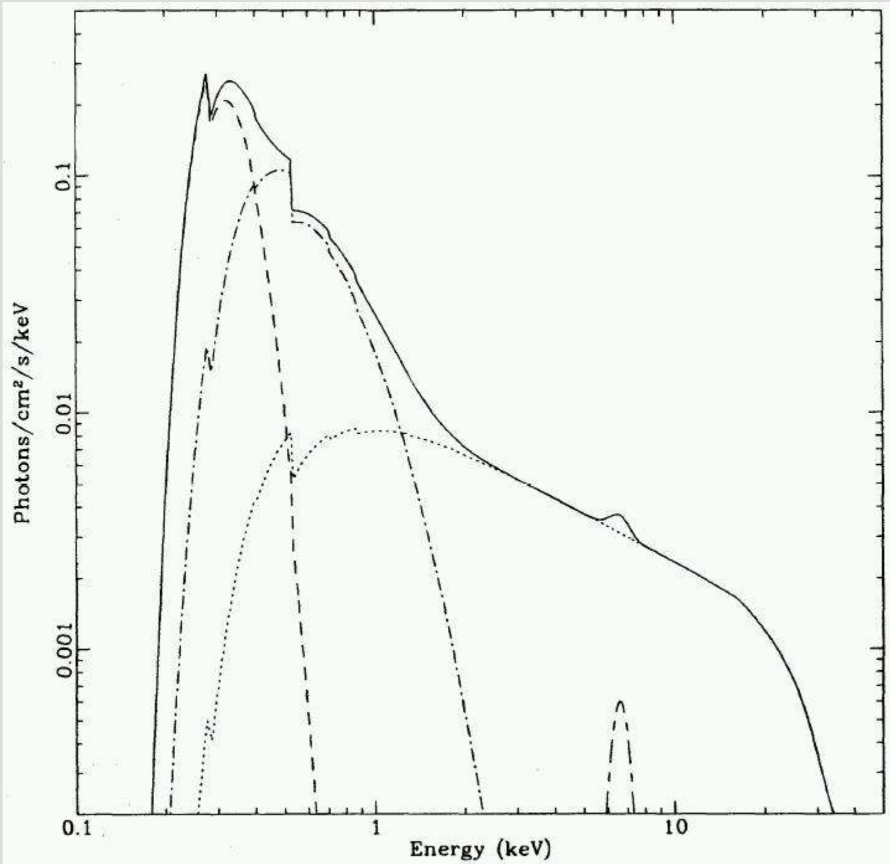

GINGA+ROSAT - Woo et al., 1996:
PL+BB+TB
kT_{BB} = 0.03 keV, kT_{TB} = 0.35 keV
L_X(2-10) = 9.3×10^{37} erg s^{-1}

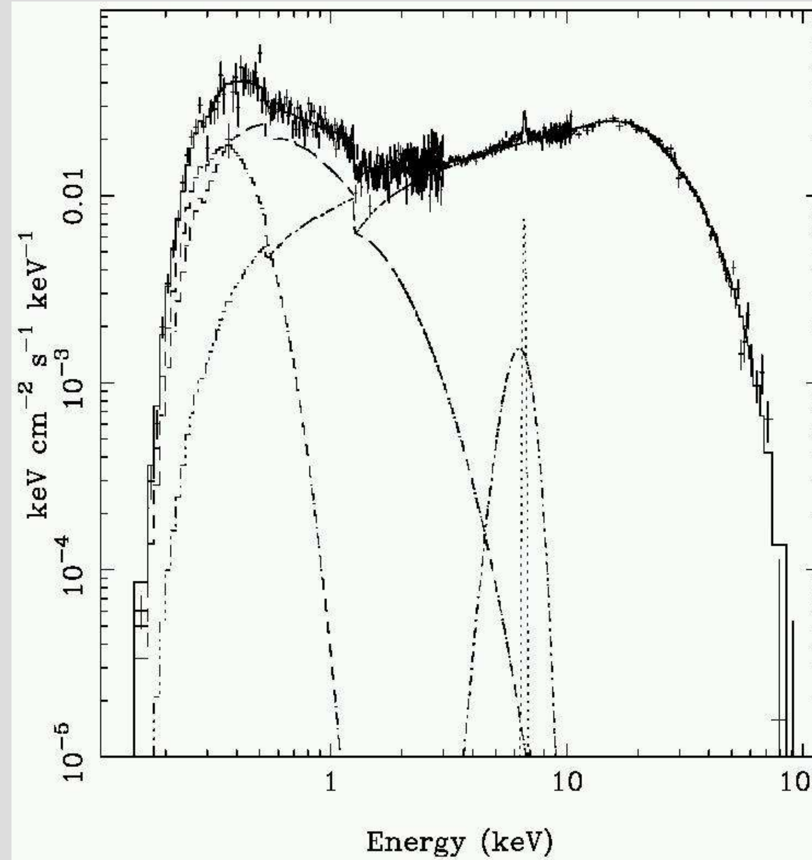

SAX - La Barbera et al., 2001:
PL+BB+BR
kT_{BB} = 0.06 keV, kT_{TB} = 0.8 keV
L_X(0.1-10) = 2×10^{38} erg s^{-1}

SMC X-1

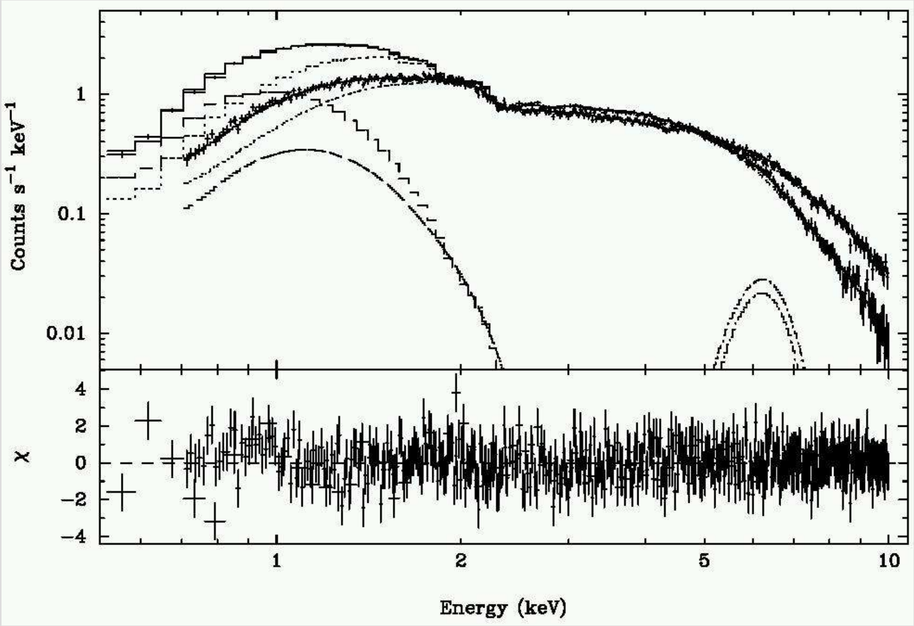

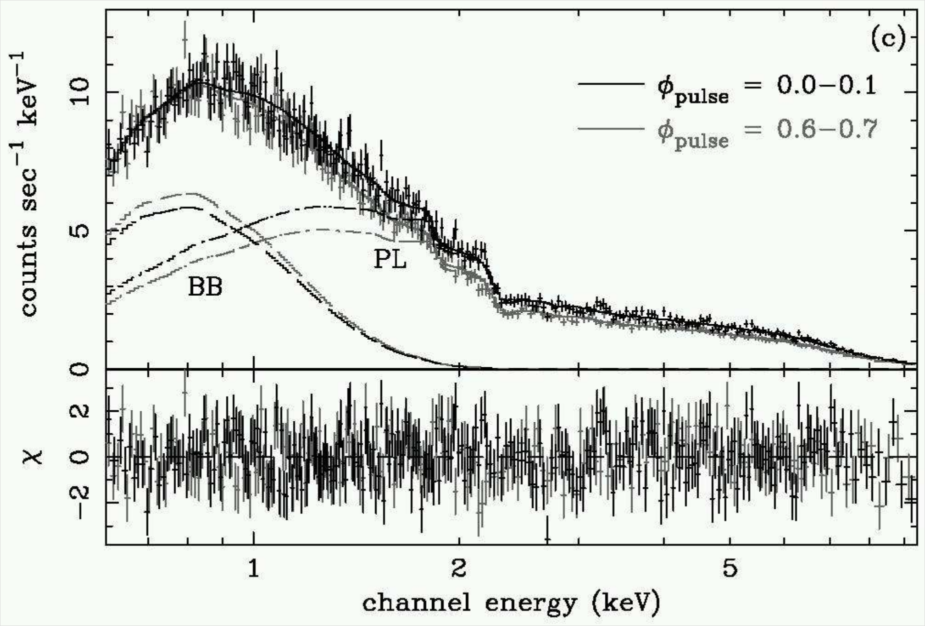

ASCA - Paul et al., 2002:
PL+BB
kT_{BB} = 0.18 keV
L_X(0.1-10) = 2.9 x 10^{38} erg s^{-1}

XMM - Hickox et al., 2005:
PL+BB
kT_{BB} = 0.17 keV
L_X(0.1-10) = 3.8 x 10^{38} erg s^{-1}

Cen X-3

EXO 053109-6609.2

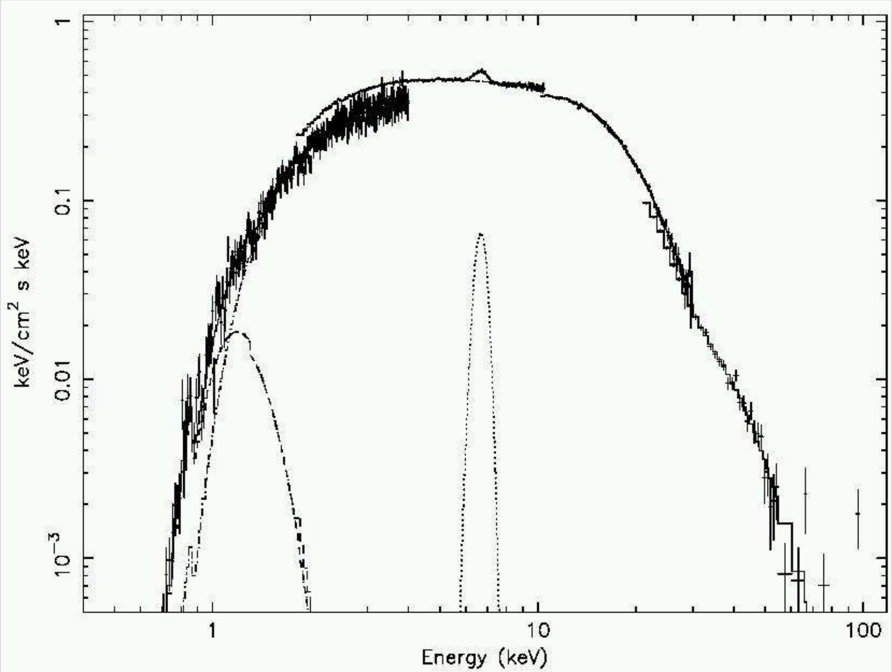

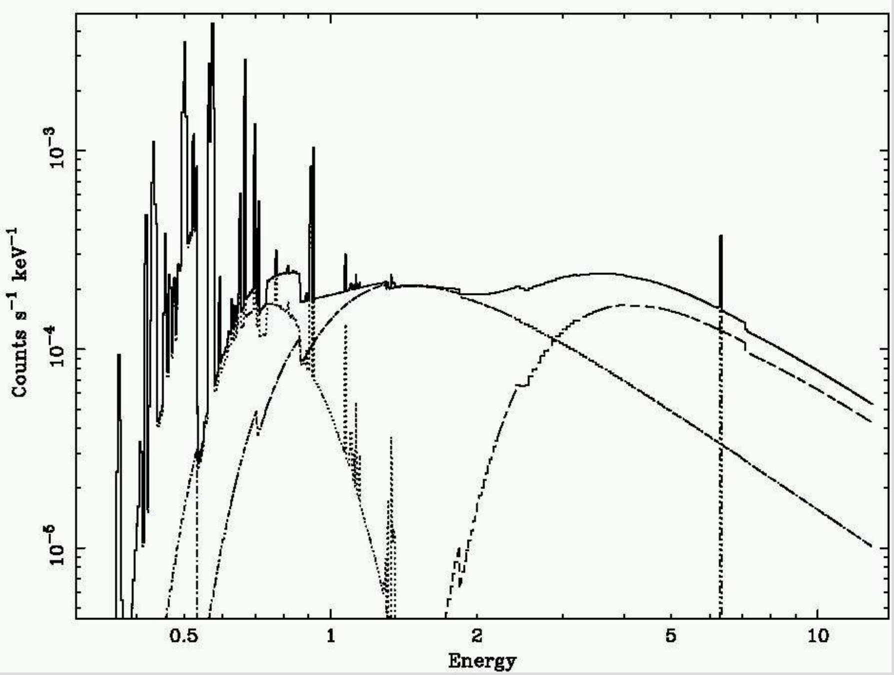

SAX - Burderi et al., 2000:
PL+BB
kT_{BB} = 0.11 keV
L_X(0.1-10) = 2.3 x 10^{38} erg s^{-1}

Haberl et al., 2003:
PL+MEKAL
kT_{MEK} = 0.1 keV
L_X(0.1-10) = 1.2 x 10^{38} erg s^{-1}

RX J0059.2-7138

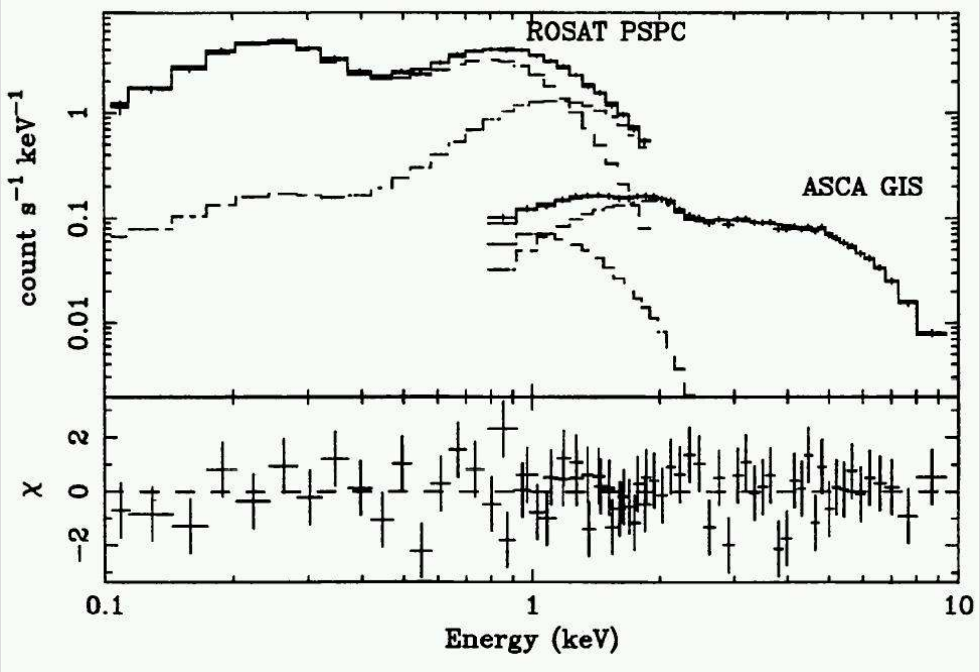

Kohno et al., 2000:
PL+MEKAL
kT_{MEK} = 0.37 keV
L_X(0.1-10) = 3.1 x 10^{38} erg s^{-1}

XTE J0111.2-7317

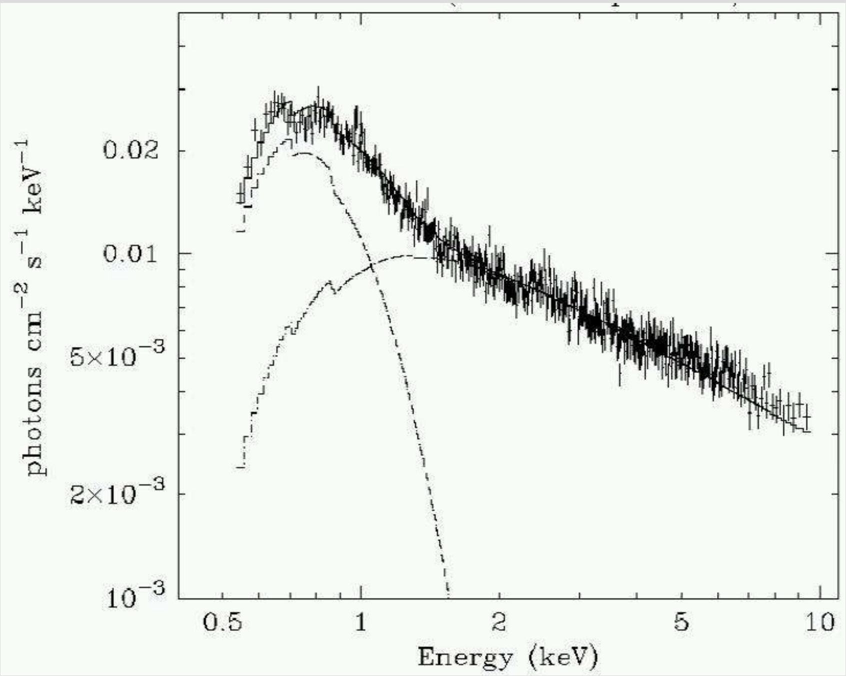

ASCA - Yokogawa et al., 2000:
PL+BB
kT_{BB} = 0.15 keV
L_X(0.1-10) = 2.5 x 10^{38} erg s^{-1}

AX J0058-720

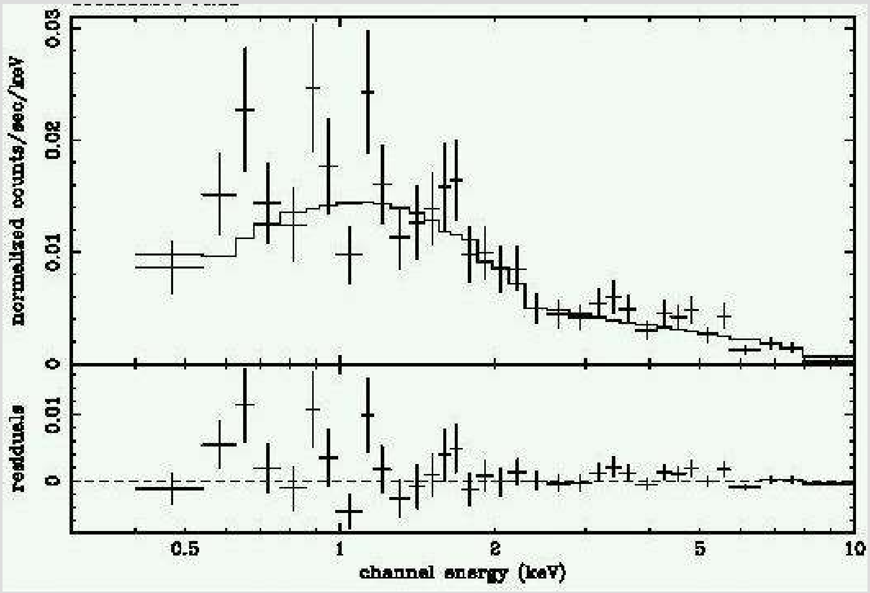

PL

$L_X(0.1\text{-}10) = 1.2 \times 10^{35}$ erg s^{-1}

AX J0103-722

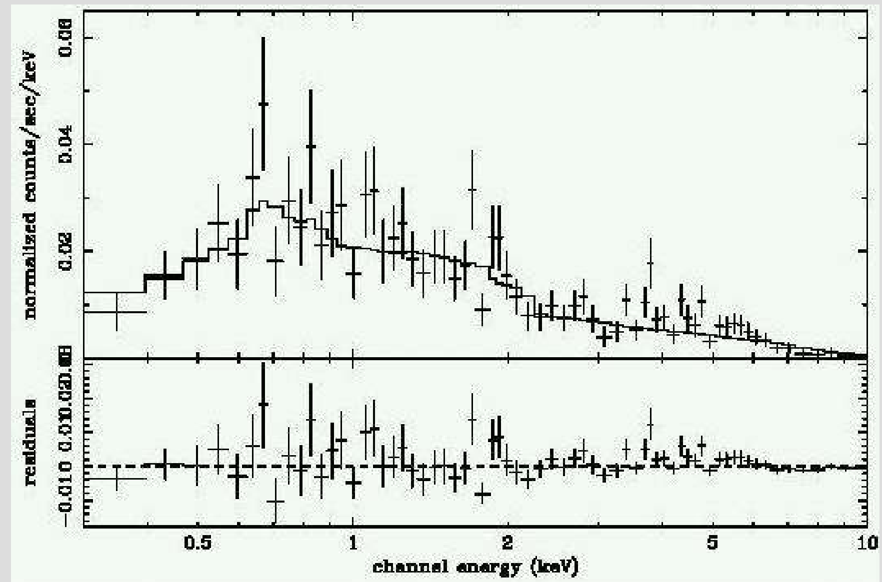

PL+MEK

$kT_{MEK} = 0.27$ keV

$L_X(0.1\text{-}10) = 3.5 \times 10^{35}$ erg s^{-1}

XMM - Sasaki et al., 2003

RX J0101.3-7211

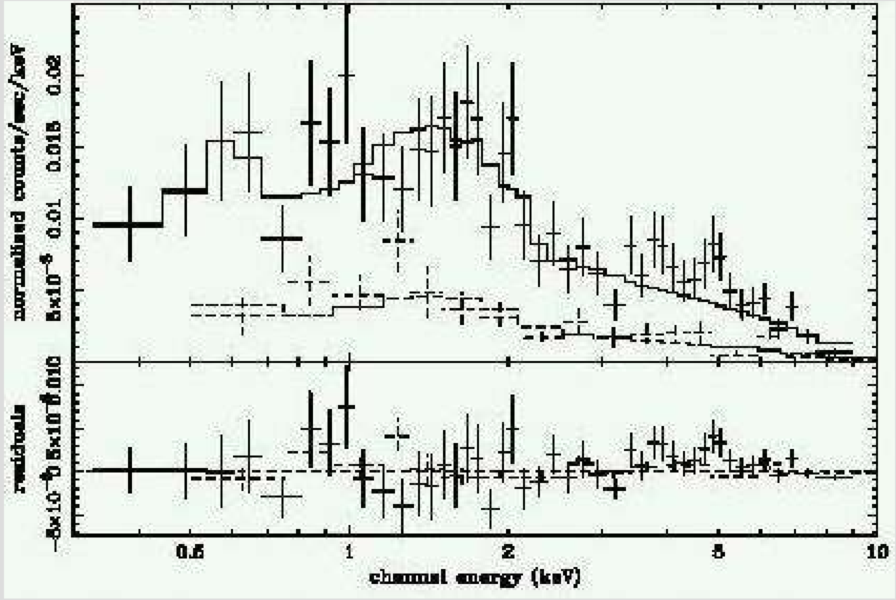

XMM - Sasaki et al., 2003:
PL+MEKAL
kT_{MEK} = 0.2 keV
$L_X(0.1\text{-}10) = 1.4 \times 10^{35}$ erg s^{-1}

RX J0103.6-7201

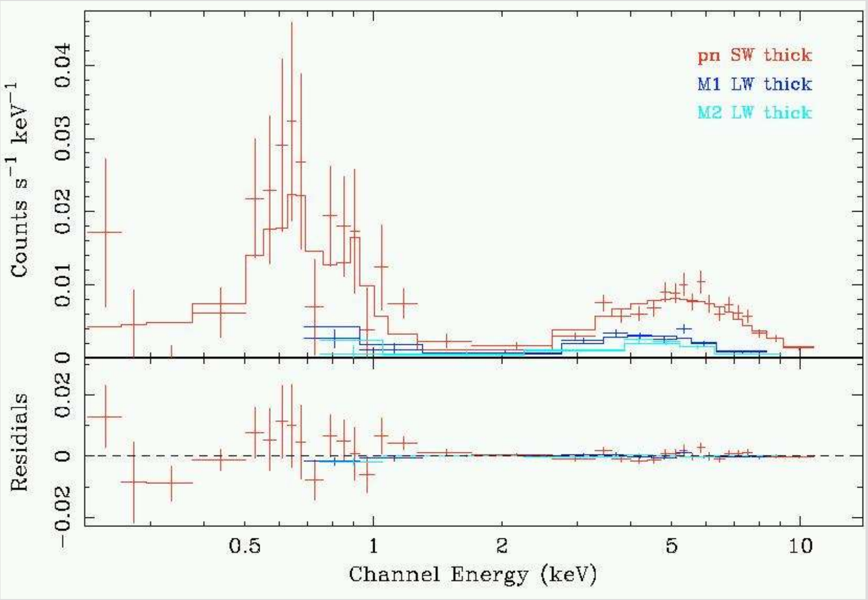

XMM - Haberl et al., 2005:
PL+MEKAL
kT_{MEK} = 0.15 keV
$L_X(0.1\text{-}10) = 1.1 \times 10^{36}$ erg s^{-1}

EM dependence on total luminosity

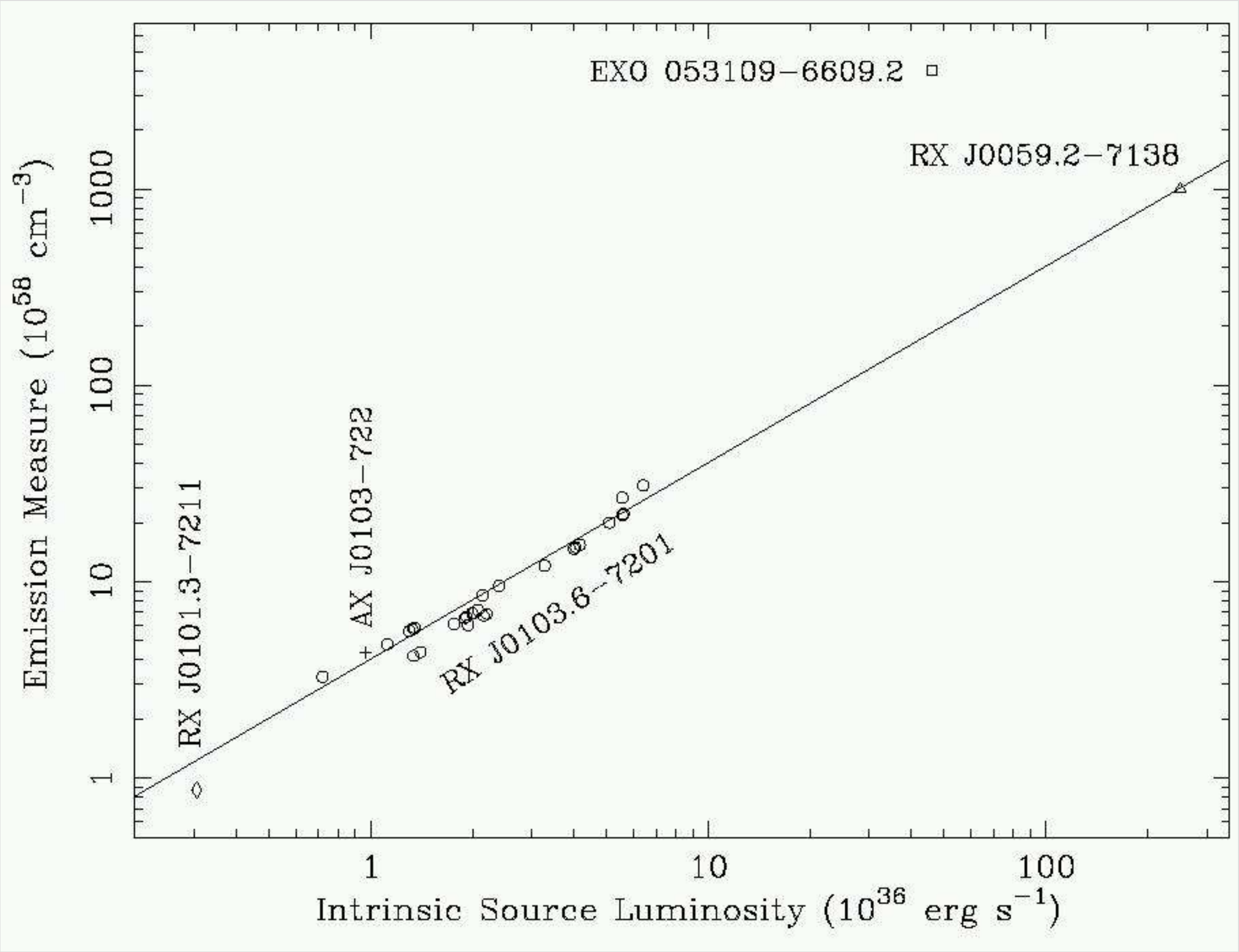

SE due to reprocessing of primary radiation?

Haberl et al., 2005

The SFXT IGR J11215 5952

Spectrum	N_H (10^{22} cm^{-2})	Γ	E_c (keV)	kT_{bb} (keV)	R_{bb} (km)	Flux (10^{-11} erg cm^{-2} s^{-1})	red. χ^2 (dof)
Cut-off powerlaw							
A1	0.62 ± 0.04	0.60 ± 0.11	11^{+4}_{-2}	–	–	6.7	1.29 (532)
A2	0.56 ± 0.04	0.25 ± 0.10	$7.3^{+1.3}_{-1.0}$	–	–	9.9	1.18 (589)
B1	0.71 ± 0.11	0.0 ± 0.23	$4.1^{+1.1}_{-0.7}$	–	–	0.5	0.99 (427)
B2	0.79 ± 0.07	0.0 ± 0.15	$4.8^{+0.8}_{-0.6}$	–	–	1.3	1.08 (574)
Powerlaw plus blackbody							
A1	$0.73^{+0.07}_{-0.06}$	$1.23^{+0.22}_{-0.16}$	–	$2.0^{+0.2}_{-0.3}$	0.24 ± 0.03	6.7	1.29 (531)
A2	0.64 ± 0.05	$0.89^{+0.11}_{-0.09}$	–	1.7 ± 0.2	0.37 ± 0.05	10	1.19 (588)
B1	$0.8^{+0.1}_{-0.2}$	$0.96^{+0.21}_{-0.39}$	–	1.4 ± 0.2	$0.14^{+0.06}_{-0.01}$	0.5	1.0 (426)
B2	$0.65^{+0.11}_{-0.07}$	0.4 ± 0.3	–	1.3 ± 0.1	0.27 ± 0.04	1.3	0.99 (573)

Sidoli et al., 2007

Possible emission processes for the data excess - I

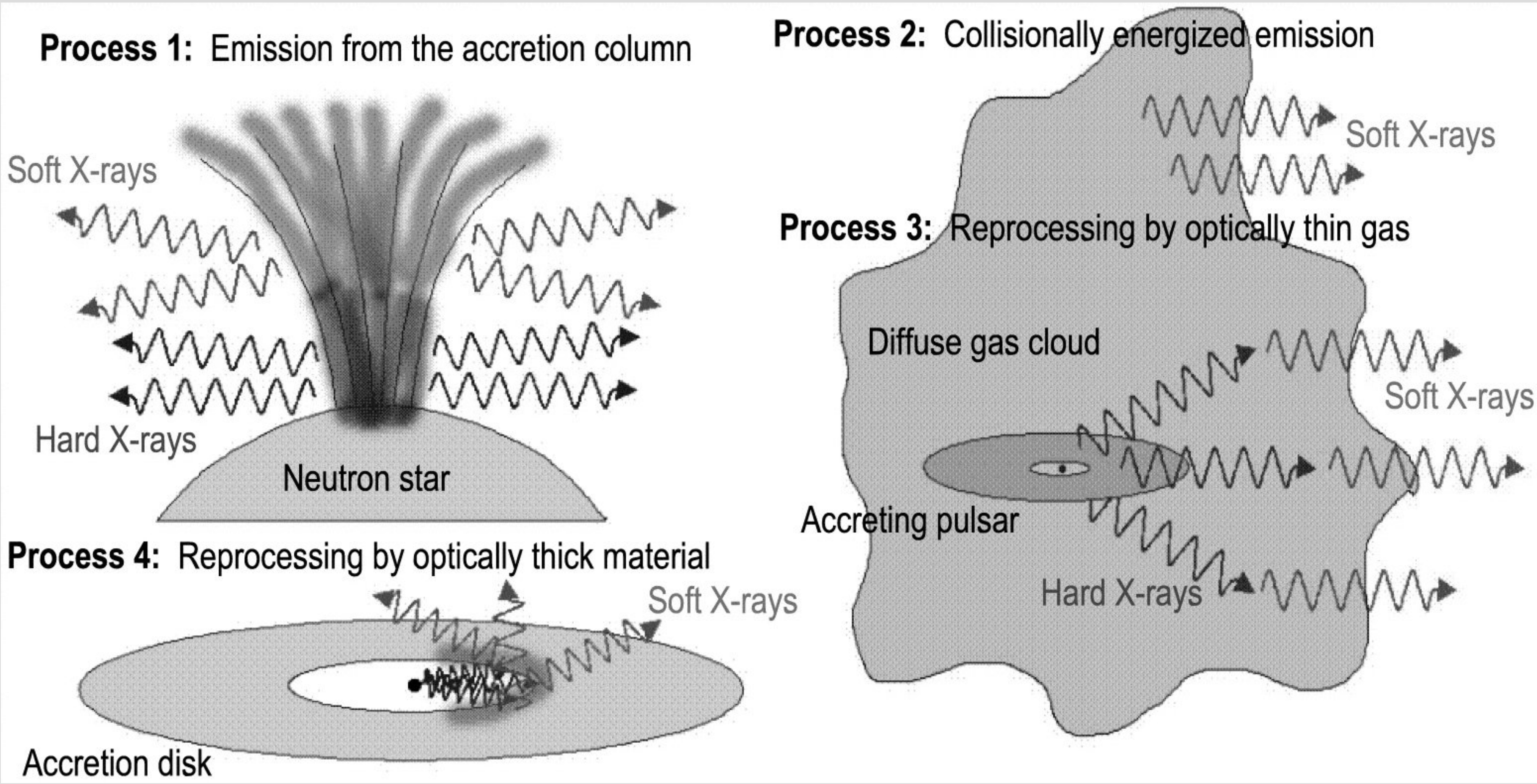

Hickox et al., 2004

Possible emission processes for the data excess - II

Hickox et al., 2004: the origin of the data excess depends on the luminosity of the source

$L_X \geq 10^{38}$ erg s^{-1}:	reprocessing of hard X-rays by the optically thick accretion material	SMC X-1, LMC X-4, Cen X-3, RX J0059.2-7138, XTE J0111.2-7317
$L_X \leq 10^{36}$ erg s^{-1}:	emission by photoionized or collisionally heated gas	Vela X-1, RX J0101.3-7211, AX J0103-722
	or	
	thermal emission from the neutron star surface	4U 1626-67, X Per
$L_X \sim 10^{37}$ erg s^{-1}:	either or both the above processes are possible	Her X-1, EXO 053109-6609.2, A0538-66

Possible emission processes for the data excess - III

Becker & Wolff, 2005: bulk Comptonization in a radiation dominated accretion column

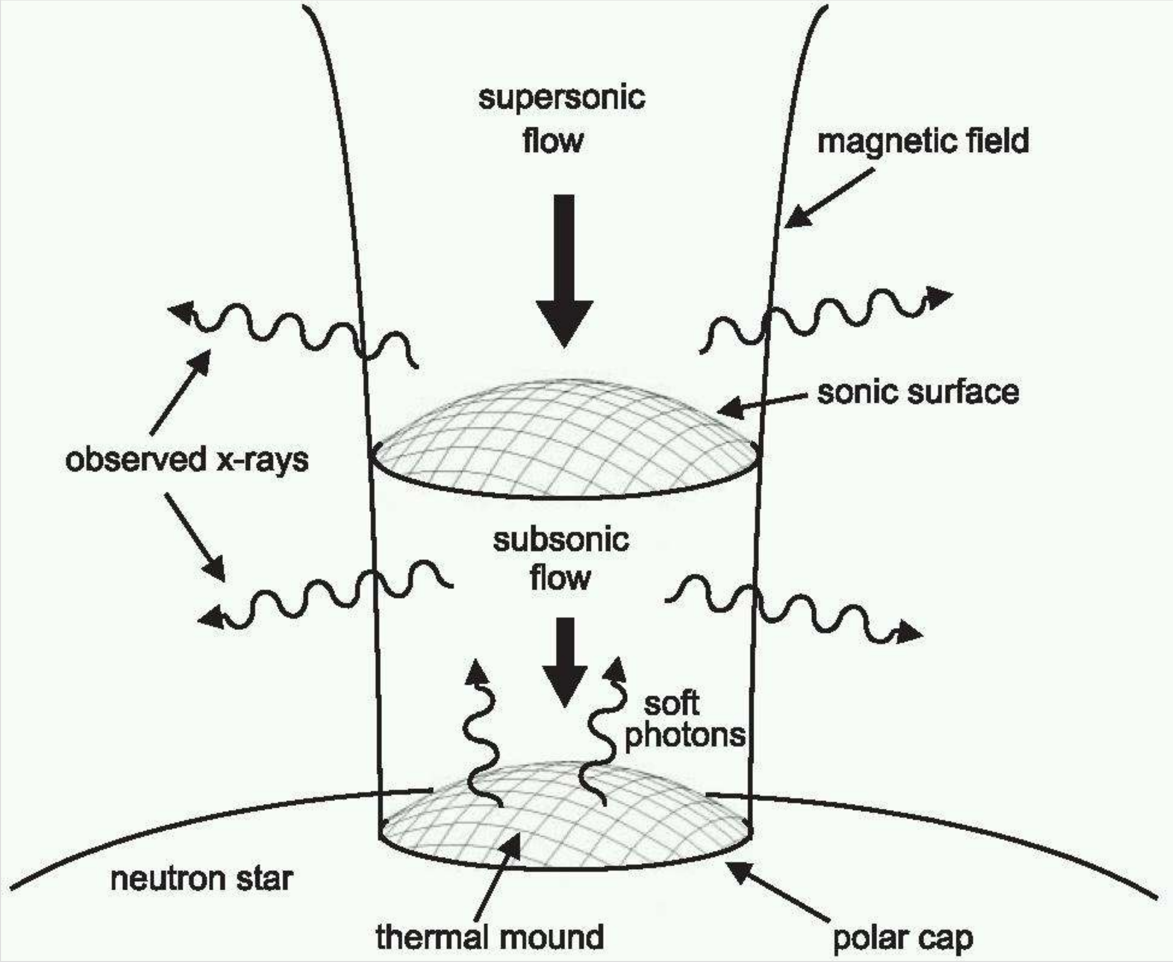

$v_{bulk} >> v_{thermal}$

↓

bulk Comptonization dominates over thermal Comptonization

$P_{radiation} >> P_{gas}$

↓

radiation dominated shock

- PL: upscattering of low-energy photons in the radiative shock and diffusion through the column walls
- BB: escape of low-energy photons without upscattering

Origin of the thermal excess in 4U 0352+309 and RX J0146.9+6121

- $L_X \leq 10^{36}$ erg s^{-1} ⇒ no reprocessing by optically thick accreting material
- the excess can be described by a black-body model ⇒ no emission by photoionized or collisionally heated gas
- the black-body temperature is high (> 1 keV)

  AND
- the emission radius is small (< 0.5 km)

⇒ thermal emission from the neutron star polar caps?

Assuming M_{NS} = 1.4 M_{SUN}, $R_{NS} = 10^6$ cm and $B_{NS} = 10^{12}$ G, we can estimate:

- the accretion rate: $dM/dt = LR_{NS} /(GM_{NS})$
- the magnetic dipole momentum: $\mu = B_{NS}R_{NS}{}^3/2$
- the magnetospheric radius: $R_m = \{\mu^4/[2GM(dM/dt)^2]\}^{1/7}$
- the accretion column radius: $R_{col} \sim R_{NS}(R_{NS}/R_m)^{1/2}$

Origin of the thermal excess in 4U 0352+309 and RX J0146.9+6121

X-ray source	4U 0352+309	RX J0146.9+6121
Luminosity (2-10 keV)	~ 10^{35} erg s^{-1}	~ 10^{34} erg s^{-1}
Accretion rate	~ 5 x 10^{14} g s^{-1}	~ 5 x 10^{13} g s^{-1}
Magnetospheric radius	~ 9.5 x 10^{8} cm	~ 1.8 x 10^{9} cm
Polar cap radius	~ 330 m	~ 230 m
Black-body radius	361 ± 3 m	140 ± 15 m

↓

the BB size is in agreement with the polar-cap origin of the thermal excess!

BUT

there is no clear evidence of the BB variability along the pulse phase.....

Soft excess variability: other results...

Her X-1: common Γ, kT_{BB}, E_{GAU}

LMC X-4: free parameters

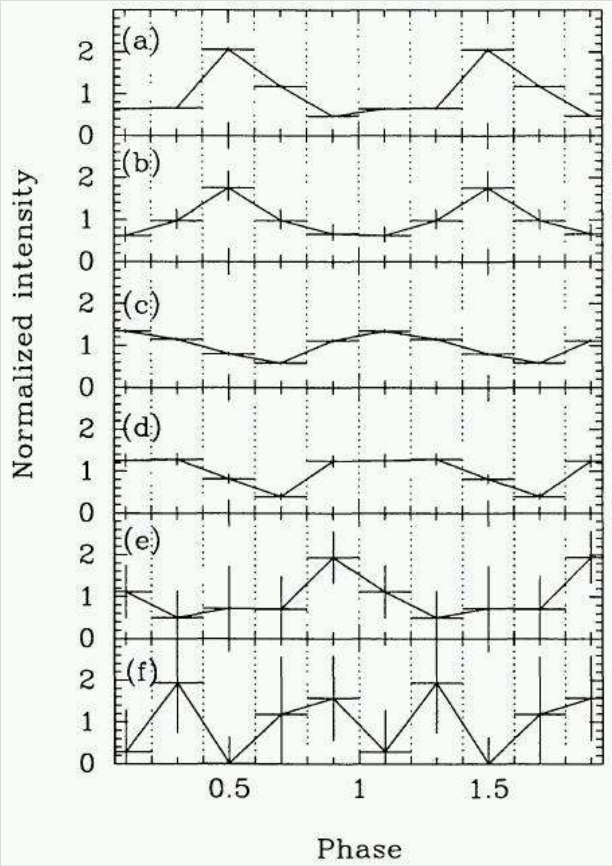

direct PL

absorbed PL

BB

gaussian @ 1keV

gaussian @ 6.4 keV

gaussian @ 6.7 keV

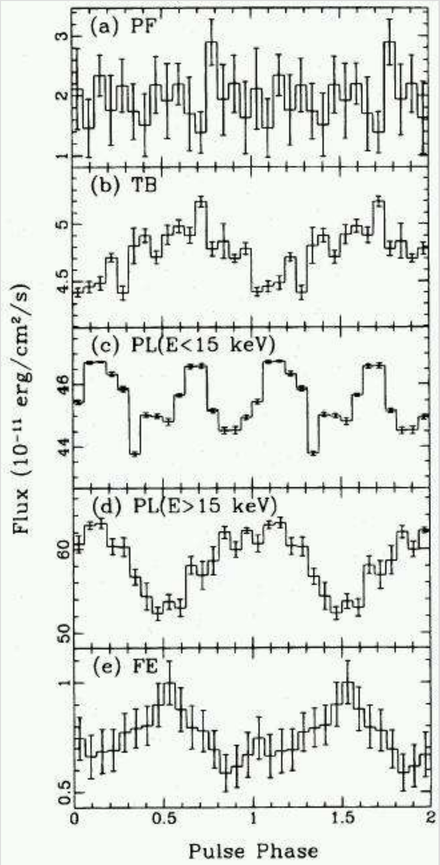

Endo et al., 2000

Woo et al, 1996

Soft excess variability: other results...

SMC X-1: free parameters

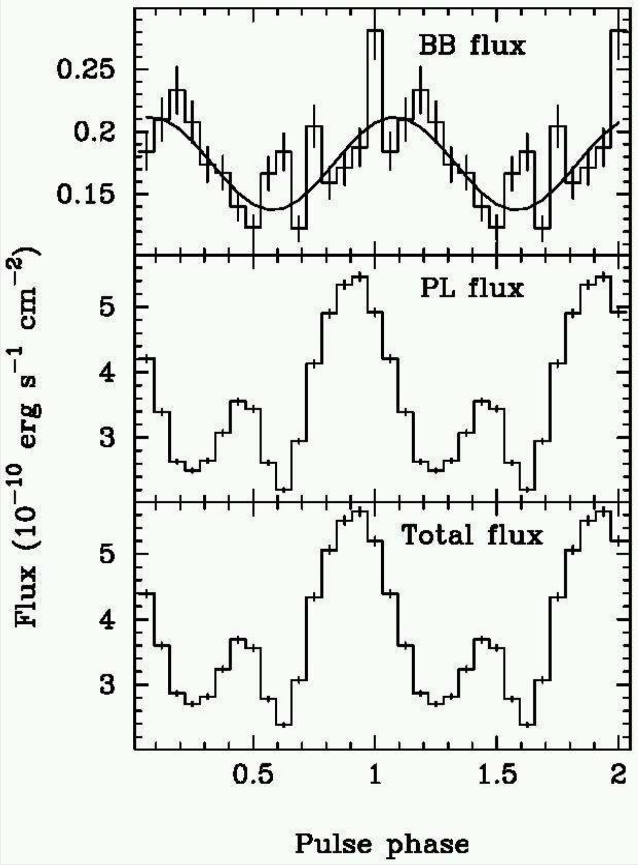

Paul et al., 2002

SMC X-1: free parameters

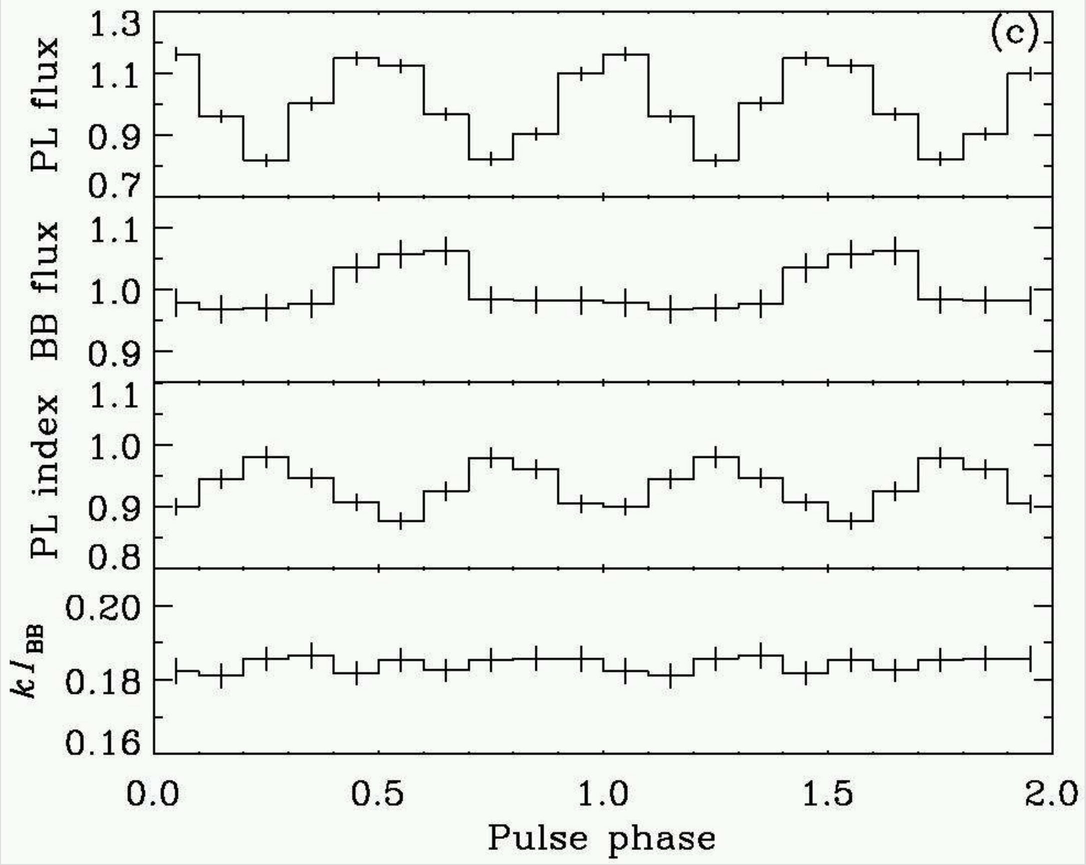

Hickox et al., 2005

Observation of the transient Be pulsar 3A 0535+262 in quiescence

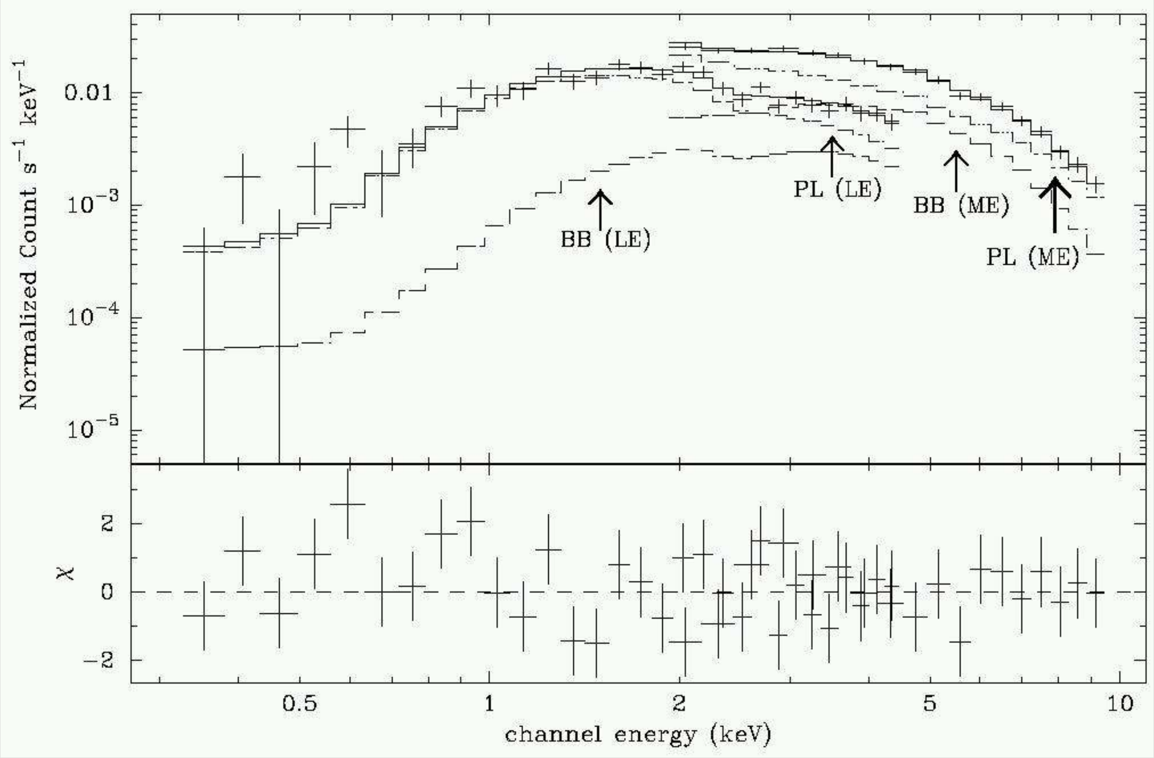

SAX, Mukherjee & Paul (2005)

Long pulse period: P_{spin} = 103.4 s

Wide orbit: P_{orbit} = 111 d

Large eccentricity: e = 0.47

$L_{TOT} = 4 \times 10^{33}$ erg s^{-1}

kT_{BB} = 1.33 keV

R_{BB} = 80 m

$L_{BB} = 1.4 \times 10^{33}$ erg s^{-1} (35 %)

↓

Is this spectral feature a COMMON property of the low-luminosity, long-period Be pulsars?

Future perspectives

4U 0352+309 and RX J0146.9+6121 are at the low L - long P end of the accreting pulsars

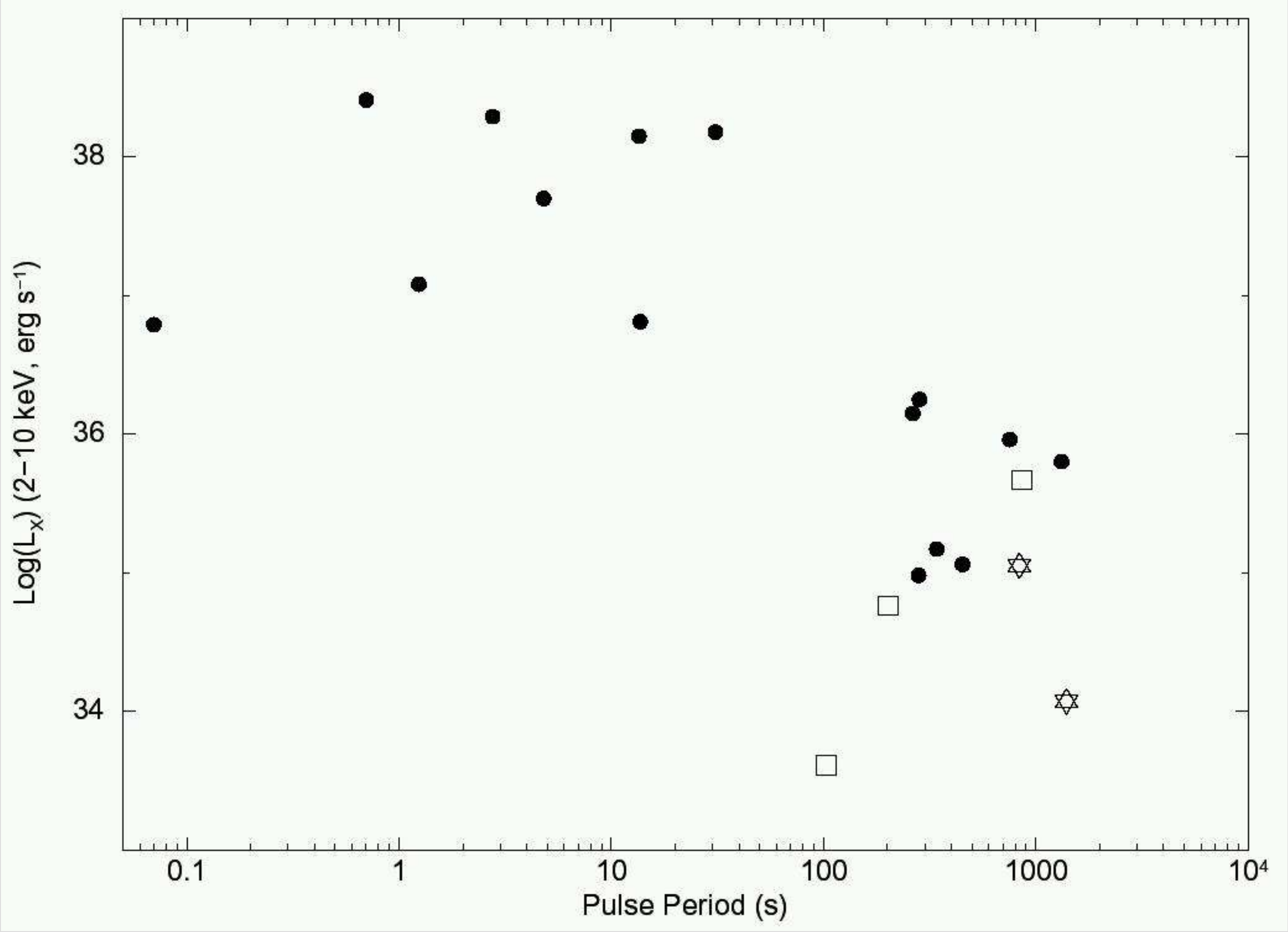

We wish to observe with XMM the other two confirmed persistent Be binary pulsars:

- RX J0440.9+4431
  P = 202 s
  $L_X \sim 2 \times 10^{34}$ erg s^{-1}
- RX J1037.5-5647
  P = 860 s
  $L_X \sim 2 \times 10^{35}$ erg s^{-1}

and also 3A 0535+262 in quiescence

proposal for XMM AO7

LET'S HOPE...

...otherwise, other types of “winds” are waiting to be studied:


CARASCO

THANKS!

P_{spin} - P_{orb} relation